

TEMPORAL DYNAMICS OF BINOCULAR DISPARITY PROCESSING WITH CORTICOGENICULATE INTERACTIONS

Stephen Grossberg[†] and Alexander Grunewald[‡]

Department of Cognitive and Neural Systems
and
Center for Adaptive Systems[§]
Boston University
677 Beacon Street, Boston, Massachusetts 02215

June, 1999

Technical Report CAS/CNS-TR-99-017
Boston, MA: Boston University

Send requests for reprints to:
Professor Stephen Grossberg
Boston University
Center for Adaptive Systems
677 Beacon Street, Boston, MA 02215
617-353-7857
steve@bu.edu

Short Title: *Cortical Binocular Disparity Dynamics*

The order of authors is alphabetical.

[†]Supported in part by the Air Force Office of Scientific Research (AFOSR F49620-92-J-0499), the Defense Advanced Research Projects Agency and the Office of Naval Research (ONR N00014-95-1-0409), the National Science Foundation (NSF IRI-97-20333), and the Office of Naval Research (ONR N00014-95-1-0409 and ONR N00014-95-0657).

[‡]Supported in part by the Air Force Office of Scientific Research (AFOSR F49620-92-J-0334 and AFOSR F49620-92-J-0225), the Defense Advanced Research Projects Agency and the Office of Naval Research (ONR N00014-92-J-4015). Present address: Division of Biology, California Institute of Technology, Mail Code 216-76, Pasadena, CA 91125.

[§]The authors wish to thank Robin Locke and Diana Meyers for their valuable assistance in the preparation of the manuscript.

Abstract

A neural model is developed to probe how corticogeniculate feedback may contribute to the dynamics of binocular vision. Feedforward and feedback interactions among retinal, lateral geniculate, and cortical simple and complex cells are used to simulate psychophysical and neurobiological data concerning the dynamics of binocular disparity processing, including correct registration of disparity in response to dynamically changing stimuli, binocular summation of weak stimuli, and fusion of anticorrelated stimuli when they are delayed, but not when they are simultaneous. The model exploits dynamic rebounds between opponent ON and OFF cells that are due to imbalances in habituating transmitter gates. It shows how corticogeniculate feedback can carry out a top-down matching process that inhibits incorrect disparity responses and reduces persistence of previously correct responses to dynamically changing displays.

Key Words: binocular vision, binocular disparity, visual cortex, lateral geniculate nucleus, neural networks, corticogeniculate feedback, binocular summation, anticorrelated stereograms, habituating transmitters, opponent processing

1 Introduction

This article develops a neural model of the temporal dynamics that occur during early stages of binocular vision. Several basic approaches toward visual neural processing have been proposed. According to one approach, neural processing occurs in a feedforward manner, whereby increasingly more sophisticated types of processing occur in a serial fashion (Celebrini, Thorpe, Trotter, & Imbert, 1993). In such a view, later processing stages do not affect earlier stages. A less radical notion uses feedback within an individual cortical area (Carandini, Heeger, & Movshon, 1997). Finally, models of cortex have been proposed that argue that feedback both within and between cortical areas plays a fundamental role in cortical processing (Hupé, James, Payne, Lomber, Girard, & Bullier, 1998; Grossberg, 1976b, 1999; Grossberg, Mingolla, & Ross, 1997).

One key argument that is often put forward to dismiss the importance of cortico-cortical and cortico-geniculate feedback is that there may not be enough time to carry out both feedforward and feedback processing, especially given that recognition can be performed in as little as 150 ms (Thorpe, Fize, & Marlot, 1996). The aim of the present article is to investigate whether known physiology and anatomy are compatible with extensive feedback processing within and between cortical areas, whether known physiological properties can emerge due to such feedback, and whether the resulting dynamic model behavior matches psychophysical data on binocular vision. We conclude first that feedback does not hinder normal visual processing, second that feedback models can account for visual psychophysical data, and third that feedback actually provides important advantages for the visual system.

The present article focuses on the temporal dynamics of *disparity* processing because this is an early and important visual process, because it has been previously claimed that the underlying timing is too tight to allow feedback to play a role (Marr, 1982), and because we have shown in an earlier study how corticogeniculate feedback connections can aid in the development of disparity selectivity (Grunewald & Grossberg, 1998). The present study focuses on disparity processing as a matter of convenience and clarity. We believe that the arguments put forward in this article are sufficiently general to be applicable in many other contexts where the role of feedback is debated.

To obtain a binocular representation of the environment, visual information available from the two eyes has to be combined. During normal viewing, the two eyes converge, and so the same part of the visual scene falls onto the centers of the two foveae. Since the two retinæ are horizontally displaced in the head, visual cues may not be registered at

corresponding locations on the two retinas. This disparity is used by the visual cortex as a powerful cue for depth (Julesz, 1971). Since objects can be at different depths, one retinal location could be paired in the cortex with several other possible locations on the other retina. The two locations that are paired typically generate a binocularly fused percept of a single location in space. One of the difficult tasks that the visual system faces is to decide which pair of retinal locations should be fused. This task is often called the *correspondence problem* (Julesz, 1971). During free viewing, human observers tend to make about three eye movements per second. This means that the correspondence problem has to be solved very rapidly based on the two images that are being processed by the two eyes. The present study explores to what extent a feedback model can account for several types of data about the transient dynamics of binocular vision that illustrate how the brain achieves this goal.

The model combines two previous modeling directions of visual perception and extends them into the dynamical domain. Both of these directions developed parts of the Boundary Contour System (BCS) of emergent boundary segmentation that was introduced by Grossberg and Mingolla (1985a, 1985b) to model aspects of the interblob cortical processing stream from the lateral geniculate nucleus (LGN) to extrastriate area V4. One modeling direction focussed on binocular vision. Grossberg (1994) further developed the BCS model by introducing FACADE theory to explain perceptual and neural data about 3-D vision and figure-ground separation. Grossberg and McLoughlin (1997) and McLoughlin and Grossberg (1998) refined FACADE theory to simulate data about da Vinci stereopsis (Gillam & Borsting, 1988; Kaye, 1978; Lawson & Gulick, 1967; Nakayama & Shimojo, 1990; Wheatstone, 1838) and about dichoptic masking, contrast-sensitive binocular matching, and Panum's limiting case (Smallman & McKee, 1995; McKee, Bravo, Taylor, & Legge, 1994b). These simulations used model interactions from LGN ON and OFF cells to cortical simple and complex cells. In a parallel development, Gove, Grossberg, and Mingolla (1995) studied a monocular version of the model that included feedback interactions from endstopped cortical complex cells back to the LGN. This work simulated data about brightness perception and the formation of illusory contours. Both of these earlier modeling directions used dynamical equations for model cells, but solved them at steady state, thereby discounting dynamic properties. The present study joins the model of Gove et al. (1995) with the binocular model of Grossberg and McLoughlin (1997) while at the same time taking dynamic properties explicitly into account.

Corticogeniculate feedback plays a key role in studies of cortical disparity tuning for several reasons. In Grossberg (1976b), it was proposed that corticogeniculate feedback car-

ries out a matching function whereby LGN cell activities that are consistent with cortical activations are preserved and synchronized, whereas inconsistent LGN activities are suppressed. In particular, monocular LGN activations were proposed to resonate synchronously with consistent cortical activations while binocularly inconsistent LGN activations are suppressed. Sillito, Jones, Gerstein, and West (1994) and Varela and Singer (1987) have reported neurophysiological evidence that is consistent with this prediction. The present work models how this feedback influences the dynamics of binocular disparity processing. Grossberg (1976b) also proposed that this corticogeniculate matching process plays a role in regulating and stabilizing the learning process whereby cortical complex cells achieve fine binocular disparity tuning during development. A recent study (Grunewald & Grossberg, 1998) models this learning process and simulates how corticogeniculate feedback may influence the development of sharp binocular tuning.

In the present study we proceed as follows: First, we review the psychophysical and physiological literature of the dynamic nature of disparity processing. Second, we outline the main processing stages of the model. Third, we give a detailed mathematical exposition of the model. Fourth, we show simulation results that show that the model is able to dynamically process disparity information, that it matches psychophysics and physiology, and that it relies on feedback. From these results, we conclude that corticogeniculate feedback plays a useful role in normal dynamic disparity processing. Some of the results have previously been reported in abstract form (Grunewald & Grossberg, 1995).

2 Review of experimental evidence

2.1 Review of neurophysiology and anatomy

Visual input from the retina projects via retinal ganglion cells to the lateral geniculate nucleus (LGN) and then to area V1 in the striate visual cortex. Area V1 is arranged in several layers (layers 1-6), and neurons in layer 6 project from area V1 back to the LGN. The following paragraphs review relevant data.

2.1.1 Retina

Ganglion cells in the retina have small receptive fields that typically consist of a central region and an annular surround (Schiller, 1992). ON cells have an on-center off-surround organization such that ON cells are excited by an increment light flash in their center, and are inhibited by an increment light flash in their surround. A decrement light flash inhibits

the center, but excites the surround. When stimulated with a uniform field they do not respond at all. OFF cells have an off-center on-surround organization that responds in the opposite way: a decrement light flash excites them in the center, and inhibits them in the surround. After the offset of a stimulus, a cell that responded to the stimulus will quickly cease to respond, while a cell of the opposite polarity, which was not activated by the stimulus, will respond briefly (Enroth-Cugell & Robson, 1966). For example, an increment light flash will excite an ON cell, and inhibit an OFF cell at the same location. At the end of the flash, the ON cell will be inhibited, but the opponent OFF cell will be transiently activated. This transient response will be called an *antagonistic rebound*.

2.1.2 Lateral geniculate nucleus

Like retinal ganglion cells, neurons in the LGN also have a center-surround structure (Wiesel & Hubel, 1966). The LGN comprises relay cells, which are excitatory and project to cortex, and interneurons that can inhibit relay cells (Sillito & Kemp, 1983). Both interneurons and relay cells receive direct input from the retina (Dubin & Cleland, 1977). When the cortico-thalamic input is abolished (e.g., by aspiration or chemical inactivation of cortex), then cells in the LGN show no orientation or length tuning (Sillito & Murphy, 1993). The effects of cortico-thalamic feedback will be discussed after a survey of cell properties in striate cortex.

2.1.3 Primary visual cortex

Area V1 in the visual cortex is arranged in six layers. Input from the LGN arrives at layer 4, where neurons have receptive fields with center-surround organization, very much like those found in the LGN. At least two different cell types have been identified in area V1: simple and complex cells. Both of these cell types are tuned for orientation, and they show spatial summation. Simple cells have clearly identifiable ON and OFF regions. If a light increment falls within the ON region, it will excite the simple cell. Likewise, a light decrement within the OFF region excites the simple cell (Hubel & Wiesel, 1962). Unlike LGN cells, however, these two regions are in general parallel, and do not surround each other (Hubel & Wiesel, 1968). An edge parallel to the border between the ON and the OFF regions of the correct polarity is the optimal stimulus for a simple cell. When a bar of optimal orientation is swept through a simple cell's receptive field, it will respond once. These properties have been discovered through neurophysiological studies of simple cells in the cat and monkey (Ferster, 1988; Liu, Gaska, Jacobson, & Pollen, 1992; Pei,

Vidyasagar, Volgushev, & Creutzfeldt, 1994). Complex cells do not have identifiable ON and OFF regions, and they respond to edges of either polarity. As a consequence, they respond twice when a bar is swept through their receptive field. This distinction between simple and complex cells has been used to define simple and complex cells (Skottun, De Valois, Grosof, Movshon, Albright, & Bonds, 1991).

Many simple cells are found in the upper parts of layer 4, and many of them are only responsive to stimulation from one eye. Complex cells are predominantly found in layers 2 and 3, and most of them are binocular. Hubel and Wiesel (1962) proposed that the cells in striate cortex are organized in a hierarchical way. According to that view, simple cells receive geniculate input and complex cells receive input from simple cells. Although this view has been challenged since then, it seems reasonable to assume that *some* simple and complex cells are arranged in this way. In support of a hierarchical emergence of a subpopulation of these cell types in area V1 is the finding that many simple cells spike shortly before complex cells spike if their receptive fields overlap and have similar orientation tuning (Alonso & Martinez, 1998). In addition, more simple cells are monocular than complex cells (Gilbert, 1977; Hubel & Wiesel, 1968), suggesting that simple cells are closer to geniculate inputs than complex cells.

All these cell types and interactions discussed thus far are considered to be excitatory. There are also inhibitory interactions, and inhibitory interneurons in the primary visual cortex. Mutual inhibition between simple cells of opposite contrast polarity has been reported (Ferster, 1988; Liu et al., 1992; Pei et al., 1994). In addition, it appears that complex cells interact via inhibitory signals within V1 (Sillito, 1979; Sillito, Salt, & Kemp, 1985). Inhibitory interactions similar to antagonistic rebounds previously discussed in the retina have also been found in cortical simple and complex cells (Ringach, Hawken & Shapley, 1997). At present it is unclear whether these rebounds are cortically generated or whether they are subcortical rebound responses that are propagated into cortex. However, it is clear that habituation at cortical synapses does occur (Abbott, Varela, Sen, & Nelson, 1997), which would allow rebound responses to be generated cortically (Grossberg, 1980). Inhibitory interneurons have a slower time constant than excitatory cells. There is evidence that suggests that pairs of excitatory and inhibitory neurons work together: the excitatory neuron excites the inhibitory neuron, and (slightly delayed) the inhibitory neurons inhibits the excitatory neuron (Krüger & Aiple, 1988). At present it is not clear how localized this inhibitory effect is.

Excitatory neurons in area V1 differ in the extent to which they respond to stimulation

by either eye or by both eyes. This is called ocular dominance. Some cells fire only if one of the eyes is stimulated, while the input in the other eye is irrelevant. Other cells fire when either eye is stimulated, and they fire stronger when both eyes are stimulated (Gilbert, 1977; Hubel & Wiesel, 1968; Ohzawa & Freeman, 1986a, 1986b).

2.1.4 Corticogeniculate feedback

The LGN also receives projections from layer 6 of the striate cortex (Robson, 1983). In fact, the majority of the input to LGN cells comes from there. The strength of this feedback projection suggests that it may play an important role in visual processing. It has been reported that cells in the LGN are endstopped, and that they can show orientation and length tuning (Cleland, Lee, & Vidyasagar, 1983), which is likely to be mediated through the cortico-thalamic projections (Sillito & Murphy, 1993). Varela and Singer (1987) and Sillito et al. (1994) showed that cortical feedback can have a pronounced effect on the excitability of cells in the LGN. Those authors found geniculate activity is reduced when the retinal input to the LGN does not match the cortical feedback. Thus corticogeniculate feedback can have a profound effect on neural activities in the LGN.

Feedback from cortex is excitatory (Montero, 1990), but it goes to both interneurons (Weber, Kalil, & Behan, 1989) and relay cells (Dubin & Cleland, 1977). Due to this complex pattern of connections, conflicting results have been reported: there are reports of excitatory influences (Kalil & Chase, 1970), inhibitory influences (Hull, 1968), and mixed effects (Marrocco & McClurkin, 1985). It seems clear from these results that feedback plays a role in spatially localized processing. Evidence to support this comes from the precise topography of the feedback projections (Updyke, 1975). This means that a simple role as the source of arousal cannot be conjectured for the feedback projections.

2.2 Review of Psychophysics

Important dynamic properties of 3-D vision are binocular summation, non-fusion of simultaneous anticorrelated stereograms, and fusion of delayed anticorrelated stereograms. They are discussed here to illustrate various facets of the dynamical interactions in visual binocular processing.

2.2.1 Binocular summation

When one views the world with only one eye, the world does not appear darker, even though the visual system is in fact receiving less visual input. This is known as Fechner's paradox (Cogan, 1982; Hering, 1964; Levelt, 1965). However, there are situations in which Fechner's paradox does not hold. In particular, when viewing very brief or very dim stimuli, the detection threshold is lower when the stimulus is seen binocularly rather than monocularly (Andersen & Movshon, 1989; Cogan, Clarke, Chan, & Rossi, 1990; Westendorf, Blake, & Fox, 1972). In other words, binocular summation affects the perception of surface properties. This result can also be extended to orientation discrimination tasks, in which subjects' performance improves when both eyes are stimulated (Bears & Freeman, 1994; Legge, 1984a, 1984b). Thus, binocular summation can also influence properties of boundary segmentation. Taken together, these findings suggest that for brief and low contrast stimuli, a facilitation occurs when stimuli are viewed binocularly as opposed to monocularly, and that such binocular summation seems to involve both surface properties, such as brightness perception, and boundary properties, such as orientation discrimination. This stimulus paradigm hereby probes the energetic aspects of binocular fusion through time. The present analysis models boundary properties. Grossberg and Kelly (1999) modeled the surface properties that lead to binocular brightness summation and Fechner's paradox.

2.2.2 Fusion of anticorrelated stereograms

A stereogram is made up of two images, one for each eye. When these images are binocularly fused, a percept in depth becomes visible. In correlated stereograms, two images are constructed with corresponding features, which may be slightly shifted to create a disparity when each picture is viewed through a different eye. Random dot stereograms are stereograms that exclusively contain black and white dots arranged in a random fashion (Julesz, 1960). This is illustrated in the top half of Figure 1. To perceive depth from such a stereogram, the visual system typically matches dots with the same contrast polarities relative to their background.

In an anticorrelated random dot stereogram, the contrast polarities between the two images are reversed. This is illustrated in the bottom half of Figure 1. It is impossible to fuse them under normal conditions (Julesz, 1960). However, if two anticorrelated pictures are presented with a slight temporal asynchrony (about 60 ms), then fusion is possible (Cogan, Lomakin, & Rossi, 1993). Afterimages occur following visual stimulation and have

reversed contrasts. This suggests that the fusion of one image occurs with the afterimage of an earlier image in the other eye. At similar asynchronies, fusion of correlated stereograms becomes impossible.

Figure 1

2.3 Relationship between physiology and psychophysics

A study has been performed that investigates the physiological responses to stimuli referred to in the psychophysics discussion. Usually disparity tuning curves are obtained by using correlated stereograms. Recently Cumming and Parker (1997) showed that when anticorrelated stereograms are used, the tuning curves are vertically inverted. This suggests that at the stage of V1, responses to anticorrelated stereograms are still present, even though perceptually they cannot be fused. It is important to note, however, that an inversion of the tuning curve means that there is no response at the preferred disparity. Thus the data of Cumming and Parker (1997) show that “spurious” responses at the wrong disparities occur in response to an anticorrelated stimulus.

3 Simulation Methods

To investigate the importance of feedback during disparity processing, we developed the model architecture that is summarized in Figures 2 and 3. This architecture is briefly surveyed before a more detailed stage-by-stage description is given. At the lowest stage, retinal information is separated into ON and OFF channel responses. This separation has shown to be useful for modeling the processing of contrast information under conditions of variable illumination (Grossberg & Todorović, 1988; Grossberg & Wyse, 1991; Pessoa, Mingolla, & Neumann, 1995). In particular, cells that obey membrane or shunting equations, and that interact as a part of an on-center off-surround network (ON cells) or an off-center on-surround network (OFF cells), are capable of discounting the illuminant, extracting Weber-law modulated ratio contrasts, and normalizing their total activities (Grossberg, 1973, 1980). ON and OFF cells are linked together by an opponent processing network, called a gated dipole (Grossberg, 1972, 1980) wherein offset of an input to an ON cell can trigger a transient antagonistic rebound in the corresponding OFF cell. The net outputs of ON and OFF cells are passed on to the LGN stage, where they are combined with feedback from complex cells.

Figure 2

Spatially offset ON and OFF outputs from the LGN that are activated by image contrasts activate, in turn, oriented simple cells in striate cortex. Excitatory ON and OFF cell output signals add up at their target simple cells. Simple cells are sensitive to a particular contrast polarity (light-dark vs. dark-light). Simple cells of like position and orientation but opposite contrast polarity compete before their rectified activities are output to the complex cell stage. Here, information about the polarity of an edge is lost by pooling signals from like-oriented simple cells with opposite contrast polarities. This pooling process also enables binocular disparity information to be extracted. The complex cell stage, in turn, sends its activity to the LGN.

Two components of the model merit special attention: the organization of the complex cell field and of the feedback from complex cells to the LGN. The complex cell field rapidly matches the information from the two eyes. Complex cells pool activities from simple cells from both eyes and of both polarities. The main issue to be understood is how complex cells can binocularly match like contrasts from the two eyes, yet have output signals that pool opposite contrast polarities. It has been proposed that activities from simple cells of the same polarity facilitate each other while opposite polarities inhibit each other, before all polarity combinations of this interaction are half-wave rectified and added to generate the final complex cell response (McLoughlin & Grossberg, 1998; Ohzawa & Freeman, 1986a, 1986b). This ensures that complex cells pool both polarities of contrast, yet only match across like polarities. As a result of summing these half-wave rectified signals, the complex cell computes a full-wave rectified, oriented filtering of the image.

Matches also occur only within a predefined distance. In other words, there is a limit to the disparities that can be fused. This limit is called Panum's limiting area in the psychophysical literature (Fender & Julesz, 1967). Many matches can be initiated within this distance by an image at each position, but typically only one succeeds in substantially activating the complex cells there. This is ensured through recurrent lateral inhibition across the complex cell field, which contrast enhances the input pattern received by the complex cells (Sillito, 1979; Sillito et al., 1985).

At the offset of an input, the complex cell field needs to be able to reset itself, in the sense that no node remains persistently active. The model circuit that connects simple cells and complex cells contains interneurons that control this reset process.

Figure 3

The second key element of the model is feedback from the complex cell stage to the

LGN stage. This feedback stabilizes the processing at the complex cell stage. Feedback occurs when the activities of the complex cells converge onto a given disparity. This means that the winning complex cells have achieved a high level of activity, and all other cells have zero activity. Output signals from the complex cell stage reach the LGN stage, where they further activate those LGN cells that feed the active complex cells, while inhibiting LGN cells that do not. One can think of the feedback activity as a confirmation, or verification, signal. When activity at the LGN stage matches the confirmation signal, the corresponding LGN cell activities are enhanced, and therefore a stronger signal is fed to the simple and complex cell stages, so that the feedback to the LGN also increases. This feedback cycle is shown below to converge rapidly to a resonant equilibrium state between mutually consistent LGN and cortical cell activities.

3.1 Model processing stages

A more precise description of model stages and mechanisms is now given. The Results in Section 4 can be read without these details. All processing stages prior to the complex cell stage are monocular, thus requiring a double complement of neural fields, one for each eye (Figure 3). To achieve maximal conceptual clarity, each processing stage models only those neural properties that are rate-limiting in explaining the data.

We use the same equations and parameters as used in Grunewald and Grossberg (1998), except that no learning takes place, and that a fully developed system (with sharp disparity tuned kernels) is used. Some notations have been changed to be more consistent throughout. A 1-D version of the model is simulated. Cell activities are governed by membrane, or shunting, equations with a hyperpolarization term (Hodgkin, 1964; Grossberg, 1973):

$$\frac{dx}{dt} = -Dx + (U - x)E - (L + x)I. \quad (1)$$

The term $-Dx$ in equation (1) is a passive decay term which ensures that, without any external input, neural activity exponentially decays to zero. Term $(U - x)E$ is the excitatory shunting term, where E denotes excitatory input to the neuron, and U is the upper bound of neural activity. Factor $U - x$ ensures that neural activity cannot rise above U , no matter how large the input E . Term $-(L + x)I$ is a shunting inhibition term, where I denotes the inhibitory activity to the neuron, and $-L$ is the lower bound of neural activity. Factor $L + x$ ensures that activity never drops below the lower bound. Half-wave rectified activities $X = \max(x, 0)$ are passed on as output signals. In the following equations $D = U = L = 1$.

All the model parameters are summarized in Table 1.

Table 1

Most kernels used in the model are Gaussians except when otherwise indicated:

$$G_o(y) = k \exp\left(-\frac{y^2}{2\sigma^2}\right), \quad (2)$$

where σ specifies the size of the kernel. All kernels used are normalized so that $\sum_y G(y) = 1$, and k is chosen accordingly. For notational convenience, the subscript o of a kernel indicates the origin of the signal with which the kernel is to be convolved. That ensures that when, within a single equation, signals from multiple sources converge, it is clear which kernel goes with which incoming signal. The size of a kernel is the number of source nodes for which the kernel contains weights. The implemented size of the kernels throughout the simulations is 17 nodes (1 centered on the node receiving the input and 8 on either side). This does not mean each kernel is actually different from zero over all the 17 nodes used. The size from a functional point of view is determined by σ .

3.1.1 Image

There are two images, left and right. Each image consists of low or high activities. The input is a bright bar that is slowly moving rightward on a background of low intensity. The disparity between the two images varies. The activity of the retinal image is denoted by I_i . At the end of this section the input images for the various simulated stimulus conditions are described.

Figure 4

3.1.2 Retinal stage

At the retinal stage, ON and OFF responses are obtained by convolving the retinal image with center and surround kernels. These cell activities, or potentials, are then half-wave rectified to yield ON and OFF signals. This is shown schematically in Figure 4. Adaptation to prolonged exposure to a stimulus is achieved by incorporating the ON and OFF signals into a gated dipole opponent processing circuit that coordinates ON and OFF responses (Figure 5). A gated dipole responds to either ON or OFF signals with an initial transient overshoot that decays, or habituates, to a sustained lower value when the input stimulus persists. Habituation is mediated by chemical transmitters that multiply, or gate, the

signals from the ON and OFF cells (see the squares in Figure 5), before the gated signals compete and the net signals are rectified. Due to the persistence of asymmetric transmitter habituation in the input channel after the input terminates, the opponent channel gets transiently activated, after which the gated dipole gradually equilibrates to its resting status. This type of opponent interaction can be extended to include not just two neurons, or two populations of neurons (Grunewald & Lankheet, 1996).

Figure 5

Stated more precisely, at the retina of each eye, there are 4 fields of neurons: 2 eyes \times 2 polarities (ON or OFF). The membrane equations for the activities r_i^+ and r_i^- at the first level of ON and OFF cell processing, respectively, are defined as follows:

$$\frac{dr_i^+}{dt} = -Dr_i^+ + (U - r_i^+)F_i^+ - (L + r_i^+)F_i^- \quad (3)$$

and

$$\frac{dr_i^-}{dt} = -Dr_i^- + (U - r_i^-)F_i^- - (L + r_i^-)F_i^+. \quad (4)$$

The excitatory (F_i^+) and inhibitory (F_i^-) feedforward activities (related directly to the image) are defined by:

$$F_i^+ = M_I \sum_k G_I^+(k-i)I_k \quad (5)$$

and

$$F_i^- = M_I \sum_k G_I^-(k-i)I_k, \quad (6)$$

where $\sigma_I^+ = 0.3$ and $\sigma_I^- = 0.9$. The kernels are shown in Figure 6a. The half-wave rectified signal that is passed on to the next level of retinal processing is defined by $P_i = M_p \max(r_i, 0)$. The signal of an ON cell is denoted by P^+ and of an OFF cell by P^- . Here G_I^+ is a narrow center Gaussian kernel, and G_I^- is a wider surround Gaussian kernel. The kernels are flipped for the OFF cells.

Figure 6

The opponent processing of ON and OFF cell signals is modulated by a chemical transmitter process that can multiply, or gate, the transmitted strength of activity towards the next level. For each location, there is a transmitter gate that obeys the equation (Grossberg, 1972):

$$\frac{dg_i}{dt} = A(B - g_i) - C(P_i + T)g_i. \quad (7)$$

In equation (7), parameter A defines the rate of transmitter accumulation, B gives the maximal level of accumulated transmitter, and C defines the rate at which the transmitter is inactivated, or habituated, by an input signal P_i . Term $P_i g_i$ says that such inactivation occurs by mass action. Parameter T denotes a background, or tonic, level of activity. This background level of activity can be interpreted as intrinsic noise within a field of neurons. The final opponent output of retinal ON and OFF cells is given by:

$$R_i^+ = M_r \max((P_i^+ + T)g_i^+ - (P_i^- + T)g_i^-, 0) \quad (8)$$

and

$$R_i^- = M_r \max((P_i^- + T)g_i^- - (P_i^+ + T)g_i^+, 0), \quad (9)$$

respectively.

A second upper index indicates which retina a cell belongs to (left or right), thus there are the following variables at this level: $R_i^{l+}, R_i^{l-}, R_i^{r+}, R_i^{r-}$. Strictly speaking, there ought to be a neuronal field between the activities P_i and R_i at which the background level activity T is added to the ON and OFF cell signals P_i^+ and P_i^- . The intermediate field is then gated by the g_i . It is assumed that these cells equilibrate more rapidly to the input than the transmitters, and hence are solved at equilibrium. This assumption reduces the number of differential equations and accordingly speeds up simulations.

The tonic activities T calibrate the sensitivity of the network to the phasic inputs P_i . They also provide the internal activity that energizes an OFF cell rebound in response to offset of an ON cell input. The tonic terms T may be implemented in several ways to realize these properties. The main requirement is that they combine with phasic inputs before the transmitter gating stage.

3.1.3 LGN stage

At the LGN stage, the retinal ON and OFF activities are fed bottom-up into model ON and OFF cells. These cells also receive excitatory and inhibitory top-down signals from complex cells, as shown in Figure 7. As noted above, corticogeniculate feedback makes a prediction about the neural patterns that the complex cell “expects” to find at the LGN level. If the bottom-up and top-down signals match, then the LGN activity that is passed on to the next stage of processing is enhanced. If the signals do not match, then the LGN signal is attenuated. These properties are achieved by combining topographically

organized excitatory feedback with non-specific inhibitory feedback (Figure 7) to capture the main effects of the LGN feedback circuit, as in Gove et al. (1995). Target cells are activated either when only bottom-up signals are active, or when both bottom-up and top-down excitatory feedback converge. If only top-down inhibitory feedback converges on a previously active cell, then that cell's activity is attenuated. This scheme is similar to the interaction between bottom-up and top-down signals that is described in Adaptive Resonance Theory, or ART (Carpenter & Grossberg, 1993; Grossberg, 1976b, 1995).

Figure 7

There are 4 fields of neurons at the LGN level: 2 eyes \times 2 polarities (ON or OFF). The membrane equations that define LGN ON and OFF activities l_i^+ and l_i^- , respectively, are as follows:

$$\frac{dl_i^+}{dt} = -Dl_i^+ + (U - l_i^+)(R_i^+ + B_i^+) - (L + l_i^+)B_i^- \quad (10)$$

and

$$\frac{dl_i^-}{dt} = -Dl_i^- + (U - l_i^-)(R_i^- + B_i^+) - (L + l_i^-)B_i^- . \quad (11)$$

The specific excitatory (B_i^+) and non-specific inhibitory (B_i^-) feedback signals from complex cells are given by:

$$B_i^+ = M_c \sum_{k,d} G_c(i - k, d) C_{kd} \quad (12)$$

$$B_i^- = \sum_{k,d} C_{kd} \quad (13)$$

The term C_{kd} denotes a signal from a complex cell at position k that is sensitive to disparity d ; see equation (29). The complex kernel G_c in (12) is shifted by 0.5 to compensate for the shift that arises in the transition from the LGN to simple cells. In other words, the grid corresponding to the complex cell activities is shifted by half a pixel with respect to the grid of the LGN cells:

$$G_c(y, d) = k \exp\left(-\frac{(y - 0.5 + ed)^2}{2\sigma_c^2}\right) \quad (14)$$

The index d denotes the disparity (which can be -3, 0, or 3) of the complex cell, $e = -1, 1$ denotes the ocularity (left or right) of the LGN to which feedback is going, and k is chosen to normalize the kernel. The kernel is shown in Figure 6.

The LGN output signal is defined as follows:

$$L_i^+ = \max(l_i^+, 0) \quad (15)$$

$$L_i^- = \max(l_i^-, 0). \quad (16)$$

A second upper index indicates which LGN a cell belongs to (left or right). Thus there are 4 types of output signals from the LGN: $L_i^{l+}, L_i^{l-}, L_i^{r+}, L_i^{r-}$.

3.1.4 Simple cell stage

At the simple cell stage, ON and OFF signals from slightly shifted positions lead to maximal excitation. By itself, convergence of excitatory ON and OFF signals could activate simple cells even in the absence of a contrast difference. This is avoided by introducing competition between simple cells of opposite polarity, as in Figure 8.

Figure 8

There are 4 fields of neurons at the simple cell level: 2 eyes \times 2 polarities (light-dark or dark-light). The responses of simple cells are built up from convolutions of the LGN cell responses with odd-symmetric kernels:

$$s_i^+ = \sum_k K_l(i - k)L_k^+, \quad (17)$$

and similarly for s^- . In (17), K_l is an odd-symmetric kernel such that:

$$K_l(y) = k \sin(y + 0.5) \exp\left(-\frac{(y + 0.5)^2}{2\sigma_l^2}\right), \quad (18)$$

where $\sigma_l = 0.3$ gives the width of the kernel, and k normalizes the kernel. See Figure 6. In this kernel, y is shifted by 0.5 so that the simple cell is positioned between a pair of LGN cells. This affords good edge localization.

Simple cell responses S_i^+ and S_i^- are derived from s_i^+ and s_i^- as follows (see Figure 8):

$$S_i^+ = M_l \max(s_i^+ + s_i^- - \alpha|s_i^+ - s_i^-|, 0) \quad (19)$$

and

$$S_i^- = M_l \max(s_i^- + s_i^+ - \alpha|s_i^+ - s_i^-|, 0), \quad (20)$$

where the upper indices stand for dark-light (+) and light-dark (−) edges, M_l is a scaling constant, and α reduces spurious responses. The activities s_i^+ and s_i^- give the contributions of the ON and OFF cells to the dark-light simple cell. Both need to be sufficiently active to fire the simple cell. The absolute value term $\alpha|s_i^+ - s_i^-|$ ensures that the simple cell does not fire when both s_i^+ and s_i^- are activated, or if only one of the two is active. This rule combines two similar simple cell models previously described (Gove et al., 1995; Grossberg & McLoughlin, 1997). Another upper index is added to (19) - (20) to denote the eye of origin (l or r): S_i^{l+} , S_i^{l-} , S_i^{r+} , S_i^{r-} .

3.1.5 Complex cell stage

At the complex cell stage there are two types of neurons: excitatory complex cells and inhibitory interneurons. The complex cells receive feedforward excitatory signals from simple cells of like orientation and both contrast polarities. Moreover, at each location there are complex cells that are sensitive to different disparities. Such a cell will be maximally activated if simple cells of the matching polarity are activated, and if the peak of activity at the simple cells is positionally shifted between the two eyes by the disparity to which the complex cell is best tuned. Simple cell activities from opposite polarities do not lead to complex cell activation. This circuit is illustrated in Figure 9.

Figure 9

The feedforward signals from simple cells, by themselves, would lead to broad disparity tuning, because the disparate inputs to complex cells come from a whole neighborhood of perceptual space. To obtain sharply tuned complex cell disparities, the activities within the complex cell field interact via inhibitory feedback signals. The model incorporates local competition across space and across disparities (Grossberg, 1994). Each cell also sends excitatory feedback to itself. Such a recurrent competitive field is summarized in Figure 10.

Figure 10

The network is designed so that only the cell population with the strongest input receives more excitation than inhibition. Recurrent interactions amplify these potentially small differences into large differences. Such a “winner-take-all” circuit may be realized using shunting interactions in a recurrent, or feedback, on-center off-surround anatomy if a suitably defined nonlinear feedback signal function is also incorporated (Grossberg, 1973, 1980). Recurrent competitive fields also have the property that they can maintain their

activation after the input has vanished so that learning can react to the winning activation pattern throughout this interval (Carpenter & Grossberg, 1993; Grossberg, 1976a; Grunewald & Grossberg, 1998; Kohonen, 1984; von der Malsburg, 1973). Such short-term activity cannot be allowed to persist indefinitely, or else the network would not be able to process future inputs. Thus the persisting activation is reset shortly after the input terminates.

This reset circuit works as follows. Slow inhibitory interneurons are paired with each complex cell (Figure 11). These interneurons are inhibited by simple cell input and excited by complex cell feedback. They in turn inhibit their partner complex cell. When simple cells are active, they excite complex cells and inhibit the corresponding interneurons. Once a complex cell winner has emerged through feedback interactions, it excites its interneuron, but the simple cell inhibition keeps the interneuron inactive. When the input shuts off, however, the simple cells cease to respond, the interneurons are no longer inhibited by them, and thus they are only excited by complex cells. As a consequence, the interneurons become active and inhibit the corresponding complex cells until both are no longer active.

Figure 11

There are 3 fields of complex cells: one each for zero, uncrossed (far), and crossed (near) disparities. The disparities that were used are 0, -3, 3. A disparity of -3 means that the left image has been shifted by -3 (3 to the left), and the right image by 3 (3 to the right). So the actual distance between corresponding points is six units. Associated with each complex cell is also an inhibitory interneuron, as in Figure 11. The equations for the excitatory complex cell activities c_{id}^+ and the inhibitory interneuronal activities c_{id}^- are as follows:

$$\frac{dc_{id}^+}{dt} = -Dc_{id}^+ + (U - c_{id}^+)(F_{id}^+ + B_{id}^+) - (L + c_{id}^+)(F_i^- + B_{id}^- + \beta c_{id}^-) \quad (21)$$

and

$$\frac{1}{\delta} \frac{dc_{id}^-}{dt} = -Dc_{id}^- + (U - c_{id}^-)f(c_{id}^+) - (L + c_{id}^-)F_i^-. \quad (22)$$

Parameter β in (21) denotes the interneuron strength. It is chosen so that activation of the inhibitory interneuron in the absence of simple cell activity leads to inhibition of complex cells. This prevents undue persistence of complex cell activation as a result of complex cell positive feedback B_{id}^+ after inputs shut off. The small parameter δ in (22) ensures that the inhibitory interneuron reacts more slowly than the complex cell.

The feedforward signals F_{id}^+ and F_i^- in (21) define the binocular disparity filter between simple and complex cells (Grossberg & McLoughlin, 1997):

$$F_{id}^+ = M_c^f \left| \sum_k G_{s_{l-}}^+(k-i, d) S_k^{l-} + \sum_k G_{s_{r-}}^+(k-i, d) S_k^{r-} - \sum_k G_{s_{l+}}^+(k-i, d) S_k^{l+} - \sum_k G_{s_{r+}}^+(k-i, d) S_k^{r+} \right| \quad (23)$$

and

$$F_i^- = M_c^f \left| \sum_k G_{s_{l-}}^-(k-i) S_k^{l-} + \sum_k G_{s_{r-}}^-(k-i) S_k^{r-} - \sum_k G_{s_{l+}}^-(k-i) S_k^{l+} - \sum_k G_{s_{r+}}^-(k-i) S_k^{r+} \right|, \quad (24)$$

where $||$ denotes the absolute value and M_c^f scales the strength of feedforward activities. The difference within each absolute value expression ensures that maximal activation occurs when simple cells of the same polarity are active in the two eyes, as shown in the bottom half of Figure 9. If the polarities differ, only a weak signal can be generated. The absolute value operation, on the other hand, performs a full-wave rectification which ensures that the feedforward signal does not depend on what polarity the simple cells have. Each of these full-wave rectification terms may be interpreted as arising from the sum of two half-wave rectification terms that respond to one or the other polarity match, but not both, before the results are pooled at the complex cells; see Grossberg and McLoughlin (1997). In other words, feedforward activities are designed so that only simple cell activities of the same polarities can fuse, but at the same time the complex cell output pools opposite contrast polarities, which has been viewed as a defining characteristic of complex cells (Hubel & Wiesel, 1962; Gilbert, 1977; Skottun et al., 1991). This property is illustrated in Figure 9. For complex cells at zero disparity ($d = 0$), the feedforward weight M_c^f is scaled by a factor of 1.05 times its value for non-zero disparity cells. This factor ensures that, during monocular presentation, cells at the zero disparity level respond maximally.

The feedforward inhibitory Gaussian kernels G^- in (24) are not disparity tuned. They are characterized by parameter σ_s^{f-} , as in equation (2). The feedforward excitatory kernels G^+ in (23) are disparity tuned. The left and right kernels are given by:

$$G_{s_l}^+(y, d) = G(y - d) \quad (25)$$

$$G_{s_r}^+(y, d) = G(y + d) \quad (26)$$

with $\sigma_s^{f+} = 0.3$, where d gives the disparity shift of a given complex cell. As noted above, the disparities that are used in these simulations are -3, 0 and 3. Since $G(y)$ is a Gaussian that is centered on 0 as in equation (2), $G_{s_l}^+$ peaks at $y = d$ and $G_{s_r}^+$ peaks at $y = -d$. For $d = 3$, this means that the left kernel is shifted rightwards, and the right kernel is shifted leftwards; i.e., $d = 3$ corresponds to crossed disparities. Similarly, $d = -3$ corresponds to uncrossed disparities, and $d = 0$ corresponds to zero disparity. The convolution with these kernels in equation (23) implies that the input to a given complex cell will be maximal when the simple cell activities from the two eyes not only have the same polarity, but are also offset by the correct amount. When the disparity of a kernel does not match the disparity of simple cell activities (and therefore of contrast edges in the image), that particular complex cell will not survive the feedback competition defined by (21).

The feedback signals that realize the competition in equation (21) are given by:

$$B_{id}^+ = M_c^b \sum_{j,e} G_c^+(j-i)f(c_{je}^+) \quad (27)$$

and

$$B_{id}^- = M_c^b \sum_{j,e} G_c^-(j-i)f(c_{je}^+), \quad (28)$$

where M_c^b scales the strength of feedback interactions. Feedback activities are also not disparity tuned.

The feedback signal function in (22), (27) and (28) is a faster-than-linear nonlinearity $f(x) = x^4$ in order to achieve winner-take-all dynamics (Grossberg, 1973). The feedback kernel parameters σ_c^{b+} and σ_c^{b-} are given in Table 1. The profiles of all kernels are shown in Figure 6.

The output of the complex cell stage is defined by

$$C_{id} = f(c_{id}^+). \quad (29)$$

These signals represent the output of the model, and they are also the corticogeniculate feedback terms in the LGN equations (12) and (13).

3.2 Implementation details

Each field of neurons has the same size. In the present simulations, a field of 100 units was used. The units were arranged in a ring, so that no problems occur due to edge effects. All differential equations were integrated using the fourth order Runge–Kutta method, with a step size of $H = 0.01$. We equated a time step of 0.01 to one simulated millisecond. Update of the network was performed so that only values from the previous processing time step were used in calculations. Simulations were implemented as a *C* program running on Sun and SGI workstations. Table 1 summarizes all the parameters that were used in the simulations.

In all simulations the same parameters and equations were used, except in the no feedback simulations. The only differences between the simulations of the intact model are the input images.

3.2.1 Dynamic disparity response

In the simulations of normal dynamic disparity processing a bar was shown at different positions and at different disparities. The mathematical definition of the left image for $0 \leq t < 80$ ms is:

$$I_i^l = \begin{cases} 1 & 1 \leq i < 7 \\ 3 & 7 \leq i < 27 \\ 1 & 27 \leq i \leq 100 \end{cases} \quad (30)$$

and for the right image is:

$$I_i^r = \begin{cases} 1 & 1 \leq i < 13 \\ 3 & 13 \leq i < 33 \\ 1 & 33 \leq i \leq 100 \end{cases} \quad (31)$$

For $80 \text{ ms} \leq t < 160 \text{ ms}$, the mathematical definition of the left and the right image is:

$$I_i^l = I_i^r = \begin{cases} 1 & 1 \leq i < 40 \\ 3 & 40 \leq i < 60 \\ 1 & 60 \leq i \leq 100. \end{cases} \quad (32)$$

For $160 \text{ ms} \leq t < 240 \text{ ms}$, the mathematical definition of the left image is:

$$I_i^l = \begin{cases} 1 & 1 \leq i < 73 \\ 3 & 73 \leq i < 93 \\ 1 & 93 \leq i \leq 100 \end{cases} \quad (33)$$

and for the right image is:

$$I_i^r = \begin{cases} 1 & 1 \leq i < 67 \\ 3 & 67 \leq i < 87 \\ 1 & 87 \leq i \leq 100 \end{cases} \quad (34)$$

For $240 \text{ ms} \leq t < 280 \text{ ms}$ all input values are 1, in other words

$$I_i^l = I_i^r = 1. \quad (35)$$

Figure 12 represents the inputs.

3.2.2 Binocular summation

In the simulations of binocular summation a dim stimulus is presented briefly either to one eye, or to both eyes. The input is mathematically defined as follows:

$$I_i^l = \begin{cases} 1.1 & \text{if } 20 \leq i < 40 \text{ and } 0 < t < 5 \text{ ms} \\ 1 & \text{otherwise} \end{cases} \quad (36)$$

In the simulation of monocular presentation $I_i^r = 1$ for all i , whereas and in the binocular simulations $I_i^r = I_i^l$, where I_i^l is as defined above.

3.2.3 Anticorrelated stereograms

In the simulations with the anticorrelated stereogram, either an anticorrelated stereogram was shown simultaneously to both eyes, or delayed. The left input is defined as follows:

$$I_i^l = \begin{cases} 1.1 & \text{if } 20 \leq i < 40 \text{ and } 0 < t < 200 \text{ ms} \\ 1 & \text{otherwise} \end{cases} \quad (37)$$

In the simultaneous case the right input is given by:

$$I_i^r = \begin{cases} 0.85 & \text{if } 20 \leq i < 40 \text{ and } 0 < t < 200 \text{ ms} \\ 1 & \text{otherwise} \end{cases} \quad (38)$$

and in the delayed case the right input is given by:

$$I_i^r = \begin{cases} 0.85 & \text{if } 20 \leq i < 40 \text{ and } 200 \text{ ms} < t < 400 \text{ ms} \\ 1 & \text{otherwise} \end{cases} \quad (39)$$

3.2.4 No feedback

In this simulation the same stimulus as in the dynamic disparity response simulations was used, except that the corticogeniculate feedback was set to zero, i.e. $B_i^+ = B_i^- = 0$ in equations (10) and (11).

4 Simulation Results

This section shows simulations in response to the stimuli described in the previous section.

4.1 Dynamic disparity response

This simulation is used to illustrate the dynamics of each processing stage within the network. For the sequence of a bar moving in space and depth as shown in Figure 12, the responses at the various levels are shown.

Figure 12

At the retinal stage, following the onset of the first stimulus, ON and OFF responses occur at both left and right retinas. These responses rise very rapidly, and also decay rapidly, but persist during the stimulus presentation. At stimulus offset a rebound response occurs, which is slightly offset. Note, however, that the ON response and the corresponding rebound OFF response occur at the same locations. At the LGN stage, the signals from the retinal stage are made less extreme such that the initial rise is less fast, and the sustained part of the response is stronger. This occurs due to corticogeniculate feedback.

At the simple cell stage, responses only occur at the appropriate contrast transition, which then feeds into the complex cell stage. Note that the ON/OFF rebound responses

reappear in the form of DL/LD rebound responses. At the complex cell stage the appropriate disparity at the correct location is identified.

4.2 Binocular summation

In the simulations of binocular summation a brief and weak stimulus is presented either monocularly or binocularly. Figure 13 shows the responses of one cell at the complex cell stage in those two simulations. When the stimulus is monocular, the response is significantly weaker than when the stimulus is binocular.

Figure 13

With stimuli of sufficient intensity and duration, the recurrent interaction within the complex cell stage can normalize activity such that the response elicited is independent of stimulus strength. However, when the stimuli are very short and weak, complex cell stage processing is slowed down so that there is not enough time for the complex cell stage to converge before the stimulus disappears. In this regime, the presence or absence of an additional visual input, as occurs during binocular stimulation, adds sufficient energy to speed up complex cell stage processing. One could choose an arbitrary threshold as a value to be exceeded for a visual stimulus to be perceived. It then would always be possible to find a value for which the binocular stimulus causes complex cell activities to cross that value, while a monocular stimulus does not. It is in this sense that the model simulates the phenomenon of binocular summation.

4.3 Fusion of anticorrelated stereograms

Figure 14 shows the input and the complex cell activation in the anticorrelated stereogram simulations. On the left, the anticorrelated stereogram is delayed, and fusion is possible. This occurs due to the antagonistic rebound response obtained at the retinal stage after input offset. In this complementary response, polarities are inverted, but spatial positions are maintained. Because complex cells can only fuse correlated images, the rebound response of the first image can fuse with the response to the second image. In other words, the rebound response to a dark-light response is a light-dark response, which can fuse with a light-dark response due to a later stimulus. A simulation of this is shown in Figure 14. Simulations of Grunewald and Grossberg (1998) suggest that this rebound response plays a key role in controlling the development of fine disparity tuning at complex cells.

Figure 14

In contrast, when the anticorrelated stimuli are presented simultaneously, activation at the simple cell stage in the two eyes does not match. Hence, no responses at the disparity 0 occurs (the disparity in the stimulus). Instead, spurious activation occurs at other disparities and locations. Thus, the model does produce responses to anticorrelated stimuli, but the correspondence between stimulus disparity and preferred complex cell disparity is not maintained. These features have been shown physiologically (Cumming & Parker, 1997).

4.4 Responses in absence of corticogeniculate feedback

Since there is long-loop feedback from complex cells to the LGN, the dynamics of the model as a whole exhibit a greater level of complexity. Figure 15 shows the complex cell activities for the three complex cell disparities at one location when the simulation was run with and without corticogeniculate feedback.

Figure 15

In response to all stimuli, activity rises equally fast with or without feedback. Thus when only one stimulus occurs near a particular location, the presence of feedback does not delay processing. Note, however, activity in the near disparity field at a location that corresponds to the first stimulus, which appears when there is no feedback as soon as the initial response disappears. While this response is brief, it is clearly at an incorrect disparity. This occurs because, in the absence of corticogeniculate feedback, any mis-categorizations that occur at the complex cell stage are not used as a prediction to be matched against the incoming retinal stage input. Therefore this activity is not shut off.

Moreover, when feedback is present, the decay of activity at stimulus offset occurs earlier. This is due to the corticogeniculate inhibitory feedback that quenches LGN stage activities whenever no retinal stage input exists. Thus, corticogeniculate feedback helps to prevent undue persistence of geniculate and therefore complex cell stage activity. As a result, the temporal separation of subsequent visual inputs is maintained provided that inputs occur closely in space.

5 Discussion

This article shows how a model of visual processing that includes top-down corticogeniculate feedback can operate stably in the temporal domain and that feedback provides

important processing advantages for the visual system. In so doing, the model provides an alternative to modeling approaches that accept no feedback interactions between different brain areas (Celebrini et al., 1993), or feedback interactions only in the form of lateral interactions within the same brain area (Carandini et al., 1997). These results do not, however, imply that feedback is essential for all aspects of visual processing.

5.1 Modeling caveats

The present study simulates a dynamical model, but it does not incorporate many temporal parameters, such as conduction delays, synaptic delays, and various neural integration time constants. Although some estimates for these parameters are available, no agreement on precise values has been achieved. In any event, the purpose of the present model was not to argue that the model can simulate quantitative timing properties, but rather that the model is able to qualitatively explain key data about dynamic disparity processing and can stably and quickly converge on the correct disparity with the help of corticogeniculate feedback. A model of how the disparity-tuning properties that have been used herein could self-organize during a developmental critical period when the kernels G^+ in (23) are plastic was described in Grunewald and Grossberg (1998).

5.2 Relationship to motion processing

Since visual motion by definition is a dynamic visual stimulus, it would be tempting to model a variety of phenomena that combine motion and disparity with the dynamic disparity model that we have proposed here. Likely candidates would be the Pulfrich effect (Pulfrich, 1922), structure-from-motion (Bradley, Chang, & Andersen, 1998), and binocular motion aftereffects (Grunewald & Mingolla, 1998).

However, a cautionary note needs to be added. Functional differences between the visual motion system that passes through MT and the parallel visual form system that passes through V2 have been modeled, along with their interaction via the V2-to-MT pathway (Baloch & Grossberg, 1997; Francis & Grossberg, 1996; Grossberg, 1991; Qian & Andersen, 1997). The present model simulations are part of the static visual system, not the motion system. A full model of how the visual cortex responds to objects moving in depth would therefore need to analyse how static disparity interacts with motion disparity mechanisms. Based on the results developed herein, such a modeling study can now be attempted.

References

- Abbott, L. F., Varela, J. A., Sen, K., & Nelson, S. B. (1997). Synaptic depression and cortical gain control. *Science*, *275*, 220–224.
- Alonso, J. M., & Martinez, L. M. (1998). Functional connectivity between simple and complex cells in cat striate cortex. *Nature Neuroscience*, *1*(9), 395–403.
- Andersen, P. A., & Movshon, J. A. (1989). Binocular combination of contrast signals. *Vision Research*, *29*(9), 1115–1132.
- Arrington, K. F. (1994). The temporal dynamics of brightness filling-in. *Vision Research*, *34*(24), 3371–3387.
- Baloch, A., & Grossberg, S. (1997). A neural model of high-level motion processing: line motion and formotion dynamics. *Vision Research*, *37*, 3037–3059.
- Bearse, M. A., & Freeman, R. D. (1994). Binocular summation in orientation discrimination depends on stimulus contrast and duration. *Vision Research*, *34*(1), 19–29.
- Bradley, D. C., Chang, G. C., & Andersen, R. A. (1998). Encoding of three-dimensional structure-from-motion by primate MT neurons. *Nature*, *392*, 714–717.
- Carandini, M., Heeger, D. J., & Movshon, J. A. (1997). Linearity and normalization in simple cells of the macaque primary visual cortex. *Journal of Neuroscience*, *17*(21), 8621–8644.
- Carney, T., Paradiso, M. A., & Freeman, R. D. (1989). A physiological correlate of the Pulfrich effect in cortical neurons of the cat. *Vision Research*, *29*(1), 155–165.
- Carpenter, G., & Grossberg, S. (1993). Normal and amnesic learning, recognition, and memory by a neural model of cortico-hippocampal interactions. *Trends in Neurosciences*, *16*, 131–137.
- Celebrini, S., Thorpe, S., Trotter, Y., & Imbert, M. (1989). Dynamics of orientation coding in area V1 of the awake primate. *Visual Neuroscience*, *10*, 811–825.
- Cleland, B. G., Lee, B. B., & Vidyasagar, T. R. (1983). Response of neurons in the cat's lateral geniculate nucleus to moving bars of different length. *Journal of Neuroscience*, *3*(1), 108–116.
- Cogan, A. I. (1982). Monocular sensitivity during binocular viewing. *Vision Research*, *22*, 1–16.
- Cogan, A. I., Clarke, M., Chan, H., & Rossi, A. (1990). Two-pulse monocular and binocular interactions at the differential luminance threshold. *Vision Research*, *30*(11), 1617–1630.

- Cogan, A. I., Lomakin, A. J., & Rossi, A. F. (1993). Depth in anticorrelated stereograms: effects of spatial density and interocular delay. *Vision Research*, *33*(14), 1959–1975.
- Cumming, B. G., & Parker, A. J. (1997). Responses of primary visual cortical neurons to binocular disparity without depth perception. *Nature*, *389*, 280–283.
- Dubin, M. W., & Cleland, B. G. (1977). Organization of visual inputs to interneurons of lateral geniculate nucleus of the cat. *Journal of Neurophysiology*, *40*, 410–427.
- Enroth-Cugell, C., & Robson, J. G. (1966). The contrast sensitivity of retinal ganglion cells of the cat. *Journal of Physiology (London)*, *187*, 517–552.
- Fender, D., & Julesz, B. (1967). Extension of Panum's fusional area in binocularly stabilized vision. *Journal of the Optical Society of America A*, *57*, 819–830.
- Ferster, D. (1988). Spatially opponent excitation and inhibition in simple cells of the cat visual cortex. *Journal of Neuroscience*, *8*(4), 1172–1180.
- Francis, G., & Grossberg, S., (1996). Cortical dynamics of form and motion integration: Persistence, apparent motion, and illusory contours. *Vision Research*, *36*, 149–173.
- Francis, G., Grossberg, S., & Mingolla, E. (1994). Cortical dynamics of feature binding and reset: control of visual persistence. *Vision Research*, *34*(8), 1089–1104.
- Gaudio, P. (1994). Simulations of X and Y retinal ganglion cell behavior with a nonlinear push-pull model of spatiotemporal retinal processing. *Vision Research*, *34*, 1767–1784.
- Gilbert, C. D. (1977). Laminar differences in receptive field properties of cells in cat primary visual cortex. *Journal of Physiology (London)*, *268*, 391–421.
- Gillam, B., & Borsting, E. (1988). The role of monocular regions in stereoscopic displays. *Perception*, *17*, 603–608.
- Gove, A., Grossberg, S., & Mingolla, E. (1995). Brightness perception, illusory contours, and corticogeniculate feedback. *Visual Neuroscience*, *12*, 1027–1052.
- Grossberg, S. (1972). A neural theory of punishment and avoidance: II. Quantitative theory. *Mathematical Biosciences*, *15*, 253–285.
- Grossberg, S. (1973). Contour enhancement, short term memory, and constancies in reverberating neural networks. *Studies in Applied Mathematics*, 213–257.
- Grossberg, S. (1976a). Adaptive pattern classification and universal recoding, I: Parallel development and coding of neural feature detectors. *Biological Cybernetics*, *23*, 121–134.
- Grossberg, S. (1976b). Adaptive pattern classification and universal recoding, II: Feedback, expectation, olfaction, illusions. *Biological Cybernetics*, *23*, 187–202.
- Grossberg, S. (1980). How does a brain build a cognitive code? *Psychological Review*, *87*, 1–51.

- Grossberg, S. (1991). Why do parallel cortical systems exist for the perception of static form and moving form? *Perception & Psychophysics*, *49*(2), 117–141.
- Grossberg, S. (1994). 3-D vision and figure-ground separation by visual cortex. *Perception & Psychophysics*, *55*(1), 48–120.
- Grossberg, S. (1995). The attentive brain. *American Scientist*, *83*, 438–449.
- Grossberg, S. (1999). How does the cerebral cortex work? Learning, attention, and grouping by the laminar circuits of visual cortex. *Spatial Vision*, *12*, 163–186.
- Grossberg, S., & Kelly, F. (1999). Neural dynamics of binocular brightness perception. *Vision Research*, *in press*. Tech. rep. CAS/CNS-TR-98-019, Boston University, Boston, MA.
- Grossberg, S., & McLoughlin, N. (1997). Cortical dynamics of three-dimensional surface perception: Binocular and half-occluded scenic images. *Neural Networks*, *10*, 1583–1605.
- Grossberg, S., & Mingolla, E. (1985a). Neural dynamics of form perception: boundary completion, illusory figures, and neon color spreading. *Psychological Review*, *92*, 173–211.
- Grossberg, S., & Mingolla, E. (1985b). Neural dynamics of perceptual grouping: textures, boundaries, and emergent segmentations. *Perception & Psychophysics*, *38*(2), 141–171.
- Grossberg, S., & Mingolla, E., Ross, W.D. (1997). Visual brain and visual perception: How does the cortex do perceptual grouping? *Vision Research*, *20*, 106–111.
- Grossberg, S., & Todorović, D. (1988). Neural dynamics of 1-D and 2-D brightness perception: a unified model of classical and recent phenomena. *Perception & Psychophysics*, *43*, 241–277.
- Grossberg, S., & Wyse, L. (1991). A neural network architecture for figure-ground separation of connected scenic figures. *Neural Networks*, *4*, 723–742.
- Grunewald, A., & Grossberg, S. (1995). Temporal dynamics of disparity processing. *Investigative Ophthalmology and Visual Science*, *36*, 1742.
- Grunewald, A., & Grossberg, S. (1998). Self-organization of binocular disparity tuning by reciprocal corticogeniculate interactions. *Journal of Cognitive Neuroscience*, *10*, 199–215.
- Grunewald, A., & Lankheet, M. J. M. (1996). Orthogonal motion after-effect illusion predicted by a model of cortical motion processing. *Nature*, *384*, 358–360.
- Grunewald, A., & Mingolla, E. (1998). Motion after-effect due to binocular sum of adaptation to linear motion. *Vision Research*, *38*, 2963–2971.

- Hering, E. (1964). *Outlines of a theory of light sense*. Harvard University Press, Cambridge, MA.
- Hodgkin, A. L. (1964). *The conduction of the nervous impulse*. Liverpool University, Liverpool.
- Hubel, D. H., & Wiesel, T. N. (1962). Receptive fields, binocular interaction and functional architecture in the cat's visual cortex. *Journal of Physiology (London)*, *160*, 106–154.
- Hubel, D. H., & Wiesel, T. N. (1968). Receptive fields and functional architecture of monkey striate cortex. *Journal of Physiology (London)*, *195*, 215–243.
- Hull, D. H. (1968). Corticofugal influence in the macaque lateral geniculate nucleus. *Vision Research*, *8*, 1285–1298.
- Hupé, J. M., James, A. C., Payne, B. R., Lomber, S. G., Girard, P., & Bullier, J. (1998). Cortical feedback improves discrimination between figure and background by V1, V2 and V3 neurons. *Nature*, *394*, 784–787.
- Julesz, B. (1960). Binocular depth perception of computer-generated patterns. *Bell System Technical Journal*, *38*, 1001–1020.
- Julesz, B. (1971). *Foundations of cyclopean perception*. University of Chicago Press, Chicago.
- Julesz, B., & White, B. (1969). Short term visual memory and the Pulfrich phenomenon. *Nature*, *222*, 639–641.
- Kalil, R. E., & Chase, R. (1970). Corticofugal influence on activity of lateral geniculate nucleus in the cat. *Journal of Neurophysiology*, *33*, 459–474.
- Kaye, M. (1978). Stereopsis without binocular correlation. *Vision Research*, *18*, 1013–1022.
- Kohonen, T. (1984). *Self-organization and associative memory*. Springer-Verlag, New York.
- Krüger, J., & Aiple, F. (1988). Multimicroelectrode investigation of monkey striate cortex: spike train correlations in the infragranular layers. *Journal of Neurophysiology*, *60*(2), 798–828.
- Lawson, R. B., & Gulick, W. L. (1967). Stereopsis and anomalous contour. *Vision Research*, *1*, 271–297.
- Legge, G. E. (1984a). Binocular contrast summation, I. Detection and discrimination. *Vision Research*, *24*(4), 373–383.
- Legge, G. E. (1984b). Binocular contrast summation, II. Quadratic summation. *Vision Research*, *24*(4), 385–394.

- Levelt, W. J. M. (1965). *On binocular rivalry*. Institute for Perception, RVO-TNO, Soesterberg.
- Liu, Z., Gaska, J. P., Jacobson, L. D., & Pollen, D. A. (1992). Interneuronal interaction between members of quadrature phase and anti-phase pairs in the cat's visual cortex. *Vision Research*, *32*(7), 1193–1198.
- Marr, D. (1982). *Vision*. Freeman & Co., New York.
- Marrocco, R. T., & McClurkin, J. W. (1985). Evidence for spatial structure in cortical input to the monkey lateral geniculate nucleus. *Experimental Brain Research*, *59*, 50–56.
- McKee, S. P., Bravo, M. J., Taylor, D. G., & Legge, G. E. (1994b). Stereo matching precedes dichoptic masking. *Vision Research*, *34*, 1047–1060.
- McLoughlin, N., & Grossberg, S. (1998). Cortical computation of stereo disparity. *Vision Research*, *38*, 91–99.
- Montero, V. M. (1990). Quantitative immunogold analysis reveals high glutamate levels in synaptic terminals of retino-geniculate cortico-geniculate, and geniculo-cortical axons in the cat. *Visual Neuroscience*, *4*, 437–443.
- Nakayama, K., & Shimojo, S. (1990). Da Vinci stereopsis: Depth and subjective occluding contours from unpaired image points. *Vision Research*, *30*, 1811–1825.
- Ohzawa, I., & Freeman, R. D. (1986a). The binocular organization of simple cells in the cat's visual cortex. *Journal of Neurophysiology*, *56*(1), 221–242.
- Ohzawa, I., & Freeman, R. D. (1986b). The binocular organization of complex cells in the cat's visual cortex. *Journal of Neurophysiology*, *56*(1), 243–259.
- Paradiso, M. A., & Nakayama, K. (1991). Brightness perception and filling-in. *Vision Research*, *31*, 1221–1236.
- Pei, X., Vidyasagar, T. R., Volgushev, M., & Creutzfeldt, O. D. (1994). Receptive field analysis and orientation selectivity of postsynaptic potentials of simple cells in cat visual cortex. *Journal of Neuroscience*, *14*(11), 7130–7140.
- Pessoa, L., Mingolla, E., & Neumann, H. (1995). A contrast-driven and luminance-driven multi-scale network model of brightness perception. *Vision Research*, *35*, 2201–2223.
- Pulfrich, C. (1922). Die stereoskopie im dienste der isochromen und heterochromen photometrie. *Die Naturwissenschaften*, *10*, 553–564, 570–574, 596–601, 714–722, 735–743, 751–761.
- Qian, N., & Andersen R. A. (1997). A physiological model of motion-stereo integration and a unified explanation of Pulfrich-like phenomena. *Vision Research*, *37*, 1683–1698.

- Ringach, D. L., Hawken, M. J., & Shapley, R. (1997). Dynamics of orientation tuning in macaque primary visual cortex. *Nature*, *387*, 281–284.
- Robson, J. A. (1983). The morphology of corticofugal axons to the dorsal lateral geniculate nucleus. *Journal of Comparative Neurology*, *216*, 89–103.
- Schiller, P. H. (1992). The on and off channels of the visual system. *Trends in Neurosciences*, *15*, 86–92.
- Sillito, A. M. (1979). Inhibitory mechanisms influencing complex cell orientation selectivity and their modification at high resting discharge levels. *Journal of Physiology*, *289*, 33–53.
- Sillito, A. M., Jones, H. E., Gerstein, G. L., & West, D. C. (1994). Feature-linked synchronization of thalamic relay cell firing induced by feedback from the visual cortex. *Nature*, *369*, 479–482.
- Sillito, A. M., & Kemp, J. A. (1983). The influence of gabaergic inhibitory processes on the receptive field structure of x and y cells in the cat dorsal lateral geniculate nucleus (dLGN). *Brain Research*, *277*, 63–77.
- Sillito, A. M., & Murphy, J. C. P. C. (1993). Orientation sensitive elements in the corticofugal influence on centre-surround interactions in the dorsal lateral geniculate nucleus. *Experimental Brain Research*, *93*, 6–16.
- Sillito, A. M., Salt, T. E., & Kemp, J. A. (1985). Modulatory and inhibitory processes in the visual cortex. *Vision Research*, *25*, 375–381.
- Skottun, B. C., De Valois, R. L., Grosof, D. H., Movshon, J. A., Albright, D. G., & Bonds, A. B. (1991). Classifying simple and complex cells on the basis of response modulation. *Vision Research*, *31*(7/8), 1079–1086.
- Smallman, H. S., & McKee, S. P. (1995). A contrast ratio constraint on stereo matching. *Proceedings of the Royal Society (London) B: Biology*, *260*, 265–271.
- Thorpe, S., Fize, D., & Marlot, C. (1996). Speed of processing in the human visual system. *Nature*, *381*, 520–522.
- Updyke, B. V. (1975). The patterns of projection of cortical areas 17, 18, and 19 onto the laminae of the dlgn in the cat. *Journal of Comparative Neurology*, *163*, 377–396.
- Varela, F. J., & Singer, W. (1987). Neuronal dynamics in the visual corticothalamic pathway revealed through binocular rivalry. *Experimental Brain Research*, *66*, 10–20.
- von der Malsburg, C. (1973). Self-organization of orientation sensitive cells in the striate cortex. *Kybernetik*, *14*, 85–100.

- Weber, A. J., Kalil, R. E., & Behan, M. (1989). Synaptic connections between corticogeniculate axons and interneurons in the dorsal lateral geniculate nucleus of the cat. *Journal of Comparative Neurology*, *289*, 156–164.
- Westendorf, D. H., Blake, R. R., & Fox, R. (1972). Binocular summation of equal-energy flashes of unequal duration. *Perception & Psychophysics*, *12*(5), 445–448.
- Wheatstone, C. (1838). On some remarkable, and hitherto unobserved, phenomena of binocular vision. *Philosophical Transactions of the Royal Society of London*, *128*, 371–394.
- Wiesel, T. N., & Hubel, D. H. (1966). Spatial and chromatic interactions in the lateral geniculate body of the rhesus monkey. *Journal of Neurophysiology*, *29*, 1115–1156.

Captions

Table 1. The parameters used in the binocular model.

Figure 1. In a correlated stereogram (top half of figure), the left and the right images have the same contrast polarities, but the images may differ due to disparity differences between the left and the right images. In this example, all dots have zero disparity, except the two middle dots, which are slightly shifted to the left in the left image, and to the right in the right image. In an anticorrelated stereogram (bottom half of figure) the left and the right images have opposite contrast polarities, and the images may differ due to disparity differences between the left and the right images.

Figure 2. Model processing stages. The retinal stage receives visual information, extracts contrast information and passes it on to the lateral geniculate nucleus stage (LGN stage), where it is combined with corticogeniculate feedback signals. Filtering at the orientation-selective simple cell stage feeds into a disparity-selective complex cell stage. Processing is hierarchically organized, but feedback signals from the complex cell stage to the LGN stage play an important part in strengthening complex cell stage activities.

Figure 3. Detailed model architecture. The left and right images impinge on the left and right retinae respectively. The retinal stage processes contrast information using ON and OFF cells whose opponent signals are separately transmitted to the lateral geniculate nucleus stage (LGN stage), where they are combined with corticogeniculate feedback signals. The simple cell stage combines LGN stage responses to yield orientation selectivity which retains information about the polarity of image contrast. The complex cell stage pools rectified simple cell stage activities across polarities, across the two eyes, and across space. The complex cell stage binocularly matches like polarities, and also pools opposite polarities, to become selective to disparities between left and right images. The complex cell stage generates feedback signals to the LGN stage. Each rectangle corresponds to one field of 100 simulated neurons.

Figure 4. ON and OFF cells at the retinal stage. The image is convolved with center and surround kernels, which are subtracted from each other to yield ON and OFF cell responses.

Figure 5. Opponent processing of ON cells (left column) and OFF cells (right column) at the retinal stage. Transmitter inactivation leads to habituation (at squares) of the response to a persistent input. Habituation combined with inhibition between ON and OFF channels, half-wave rectified output signals, and tonic background activity result

in an antagonistic rebound response at the offset of a stimulus. The ON channel (left hand column) responds to a phasic step input on a constant tonic background (lowest left graph) by habituating its transmitter (next lowest graph). The phasic-plus-tonic ON signal is multiplied by the transmitter to generate overshoot and undershoot responses (next lowest graph). The OFF channel (right hand column) responds to only the constant tonic background (lowest right graph) which creates a constant baseline level of habituation and output (next two graphs). The habituated OFF channel output is subtracted from that of the ON channel by an opponent interaction. The result is half-wave rectified to generate a habituated, but sustained, ON response (upper left graph). When the same is done in the OFF channel, a transient antagonistic rebound occurs at the offset of the input (upper right graph).

Figure 6. The kernels used in the model. Top left: kernels at the retinal stage. Top right: feedback kernels at the LGN stage. Bottom left: kernels at the simple cell stage. Both polarities are shown (DL denotes dark-light contrast transition, and LD denotes light-dark contrast transition). Bottom right: kernels at the complex cell stage. Excitatory and inhibitory feedforward kernels (denoted by “on” and “off”), and excitatory and inhibitory feedback kernels (denoted by “back on” and “back off”) are shown. Note that only the excitatory feedforward kernels are disparity tuned. In this case the left kernel of a far tuned cell (tuned to disparity -3) is shown. The right kernel peaks at +3 (not shown). For a near tuned cell the left and right kernels are interchanged, and for a zero disparity cell both kernels peak at 0.

Figure 7. Combined bottom-up and top-down processing at the LGN stage. Feedforward signals from the retinal stage excite the LGN stage. Topographic feedback signals from the complex cell stage amplify LGN stage activities if feedforward activities match feedback activities. If there is no match, the non-specific feedback inhibition (shown on right of figure) decreases LGN stage activities.

Figure 8. The simple cell stage is excited by LGN stage ON cells and spatially displaced OFF cells (left figure). Opposite polarities at the simple cell stage are due to different spatial distributions of inputs from LGN stage ON and OFF cells. Inhibition between opposite polarities at the simple cell stage is followed by rectification to generate output signals. In response to a light-dark vertical contrast (middle figure), only one cell polarity of the pair gets activated, so an output is generated. In response to an input of spatially uniform luminance (right figure), both simple cells are equally activated and mutually inhibit one another.

Figure 9. Top: Feedforward processing at the complex cell stage. At the complex cell stage opposite polarities from the simple cell stage are pooled across space and across eyes. A cell at the complex cell stage is maximally excited if the disparity between signals at the simple cell stage matches its preferred disparity, and if activity at the simple cell stage has the same polarity. Input from the simple cell stage is arranged in a center-surround fashion, such that the cells at the simple cell stage excite nearby cells at the complex cell stage, but inhibit more distant cells. Bottom: Disparity tuning of complex cell stage. Disparity tuning at the complex cell stage is obtained by pooling activities from simple cell stage of the same polarities from the two eyes. After adding activities for each polarity, the activities corresponding to the two polarities are subtracted and then the absolute value is taken. This ensures that only cells of the same polarities can be fused, while rendering the complex cell stage insensitive to the direction of contrast.

Figure 10. Top: Feedback interactions at the complex cell stage across space. A cell excites itself, but inhibits cells that are further away in the network. Bottom: Feedback interactions at the complex cell stage across disparities. A cell excites itself, but inhibits cells that code different disparities.

Figure 11. Complex cells reset circuit interneurons. The inhibitory neuron receives the same input from the simple cell stage as the corresponding cell at the complex cell stage. In addition it is excited by that complex cell, and it inhibits the complex cell. This ensure that following cessation of input from the simple cell stage the complex cell stage rapidly ceases to be active.

Figure 12. Normal dynamic disparity processing. Activities are shown for each model stage. In this figure activities are indicated by grey values: white means high activity, black means no activity. In each sub-plot time is along the y-axis, and the location of a cell in the network is along the x-axis.

The top row shows the left and right images presented to the network. It is a white bar moving rightwards and changing disparity from far, to 0 disparity to near. The second row shows the activities at the output of the retinal stage. ON and OFF responses for left and right retinae are indicated. The third row shows the activities at the corresponding LGN stage. The fourth row shows the output of the simple cell stage, for cells selective to dark-light (DL) and light-dark (LD) contrast transition for left and right monocular cells. The final row shows the output of the complex cell stage for far cells (left), 0 disparity cells (middle), and near cells (right). The complex cell stage correctly identifies the location and the disparity of the input.

Figure 13. Simulation of binocular summation. A brief, weak stimulus is presented either monocularly or binocularly. The activities of a cell at the complex cell field at disparity 0 is shown. Note that the activities at the complex cell stage are significantly weaker in the monocular simulations compared to the binocular simulation.

Figure 14. Simulation of anticorrelated stimuli. An anticorrelated bar is presented either delayed, or simultaneously. In the delayed simulation (left group of plots) a response occurs at complex cell stage of the disparity 0, no other responses occur. In the simultaneous simulation (right group of plots) no response occurs at disparity 0, but spurious responses at near and far disparities occur.

Figure 15. Complex cell activities in the simulations with and without corticogeniculate feedback. Complex cell stage activities of individual cells of all three disparities are shown. The response rise occurs with the same delay in both cases. All responses last shorter in the presence of feedback. Moreover, incorrect responses occur when correct responses disappear (bottom row).

Parameter	Value	Description
D	1	passive decay constant of cell activity
U	1	upper limit of cell activity
L	1	lower limit of cell activity
A	0.2	rate of gate recovery
B	1	baseline gate activity
C	2	active gate decay
T	0.3	background activity
σ_I^+, σ_I^-	0.3, 0.9	width of retinal kernels
σ_c	0.6	width of corticogeniculate feedback kernels
σ_l	0.3	width of simple cell kernels
$\sigma_s^{f+}, \sigma_s^{f-}$	0.3, 5	width of feedforward complex cell kernels
$\sigma_c^{b+}, \sigma_c^{b-}$	0.1, 4	width of feedback complex cell kernels
M_I	1	coefficient of photoreceptor input
M_g	10	coefficient of ganglion input from photoreceptors
M_r	200	coefficient of LGN input from retina
M_c	4	coefficient of LGN input from complex cells
M_l	2	coefficient of simple cell signals
M_s^f	2	coefficient of feedforward complex cell signals (non-zero disparity)
M_s^f	2.1	coefficient of feedforward complex cell signals (zero disparity)
M_c^b	300	coefficient of feedback complex cell signals
α	1.3	simple cell threshold
β	20	weight of complex cell inhibitory interneuron
δ	0.5	integration speed of inhibitory interneurons

Table 1:

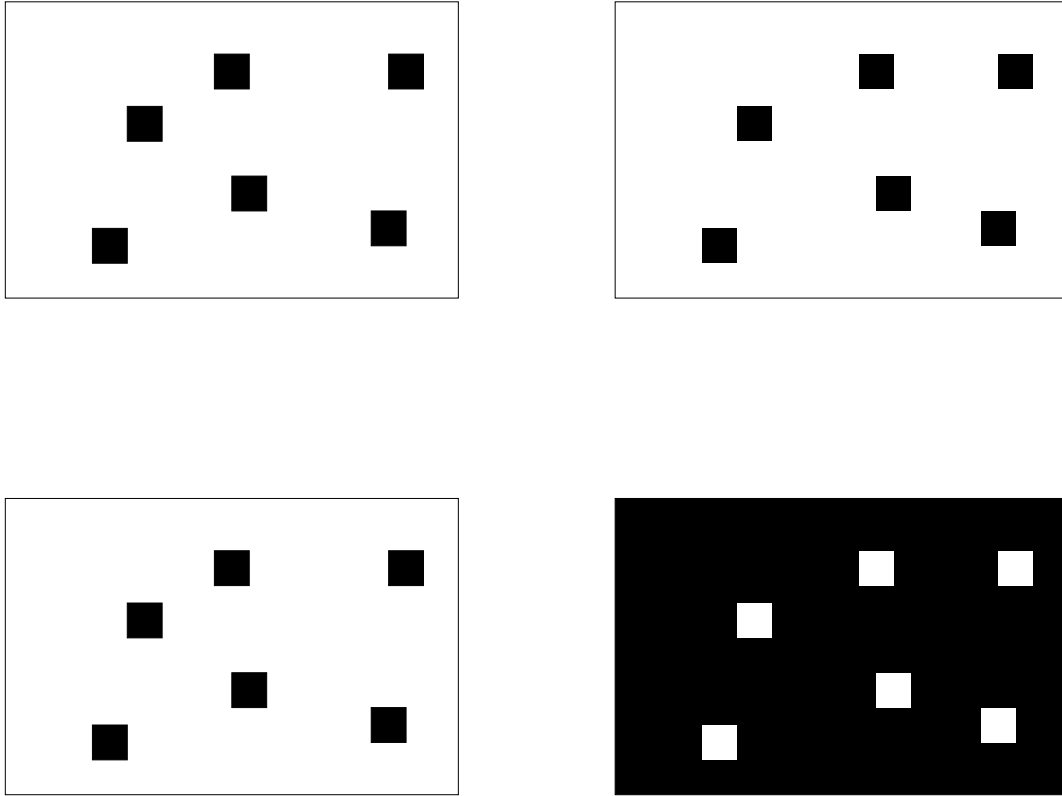


Figure 1:

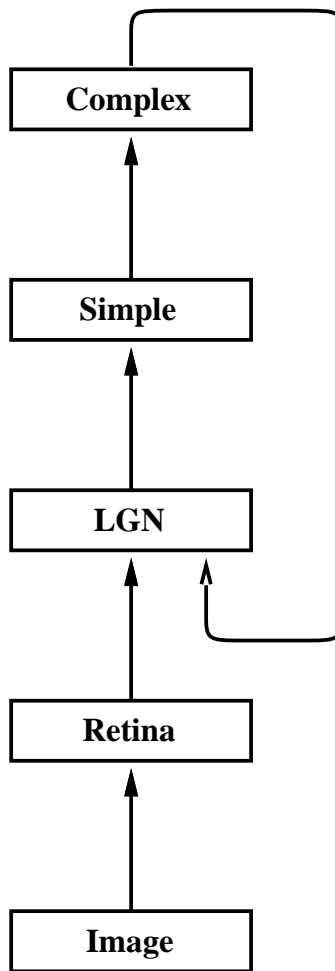


Figure 2:

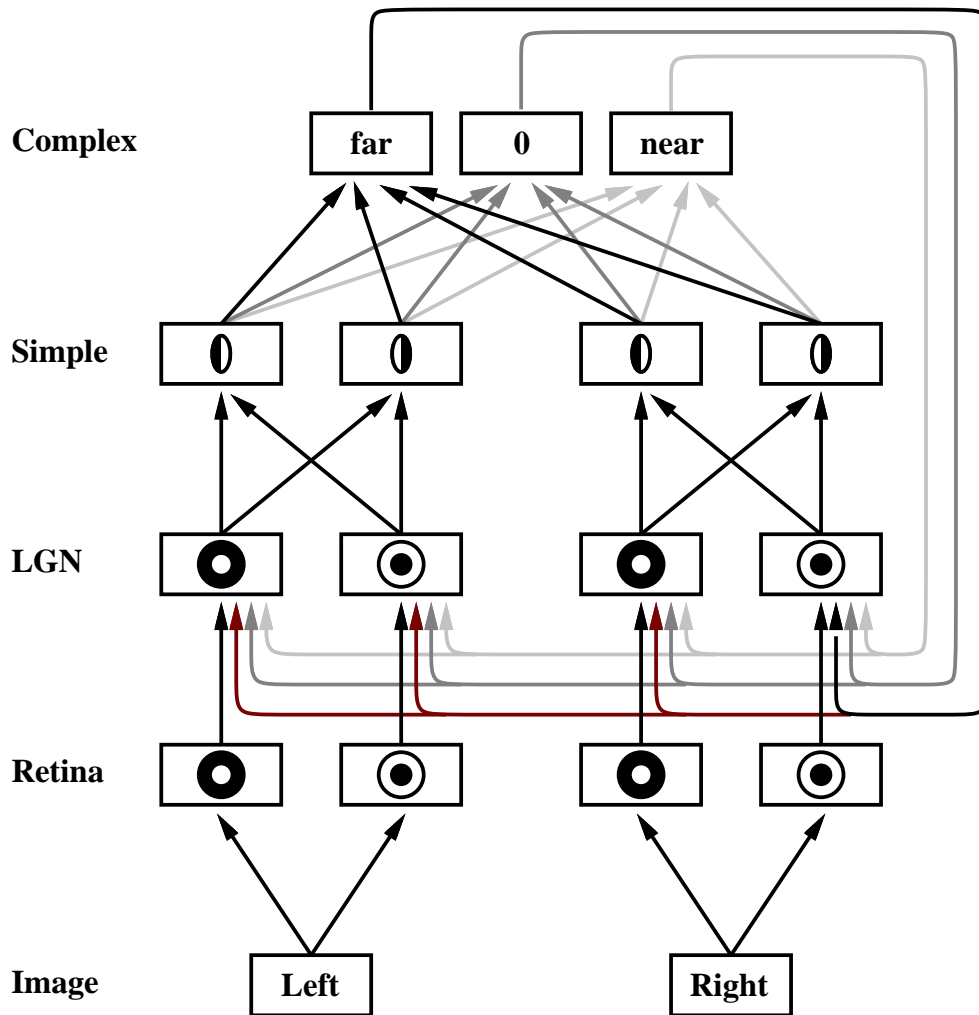


Figure 3:

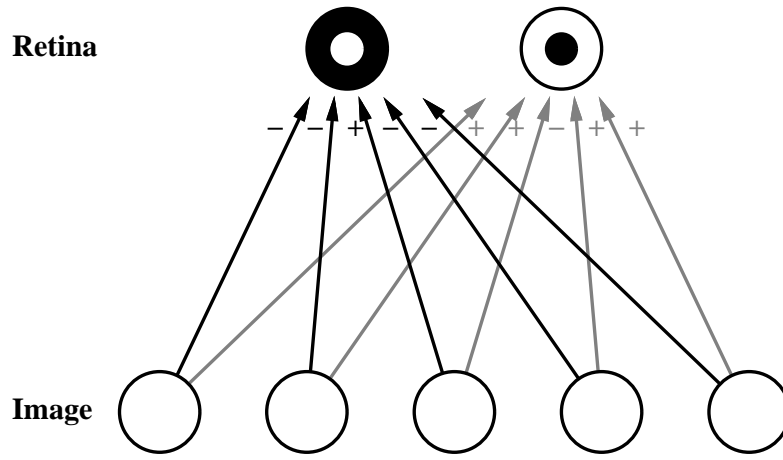


Figure 4:

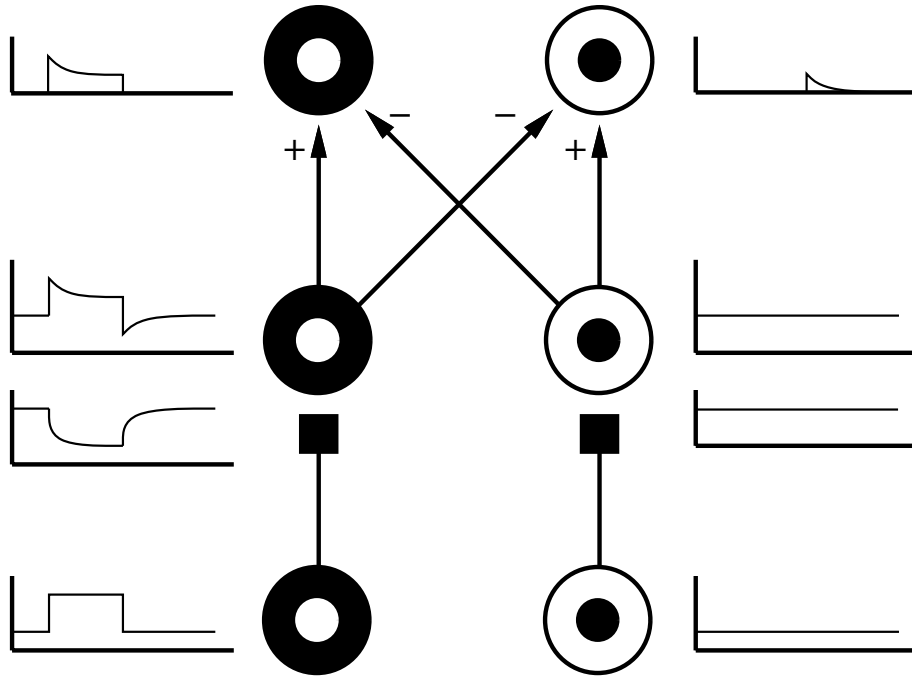


Figure 5:

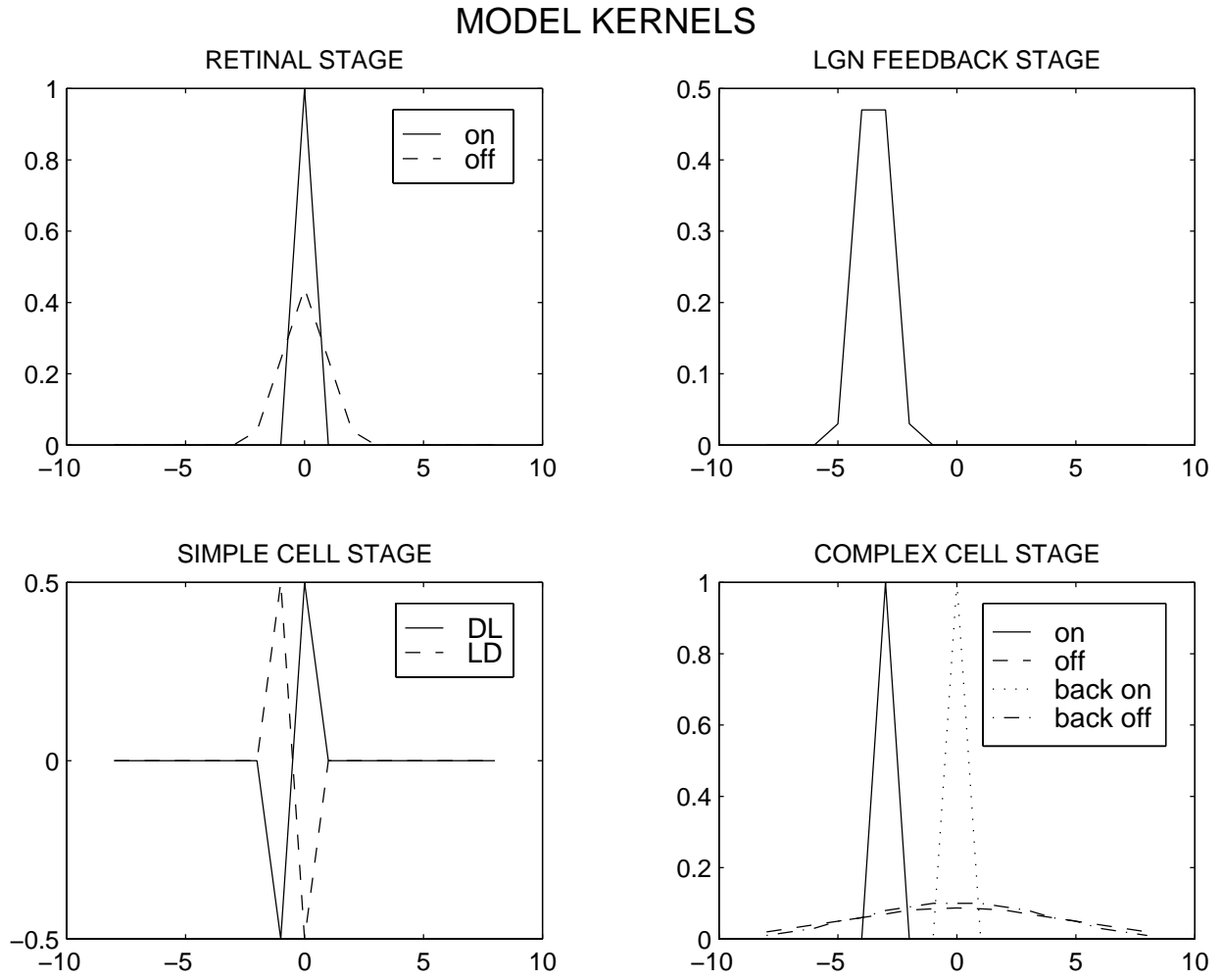


Figure 6:

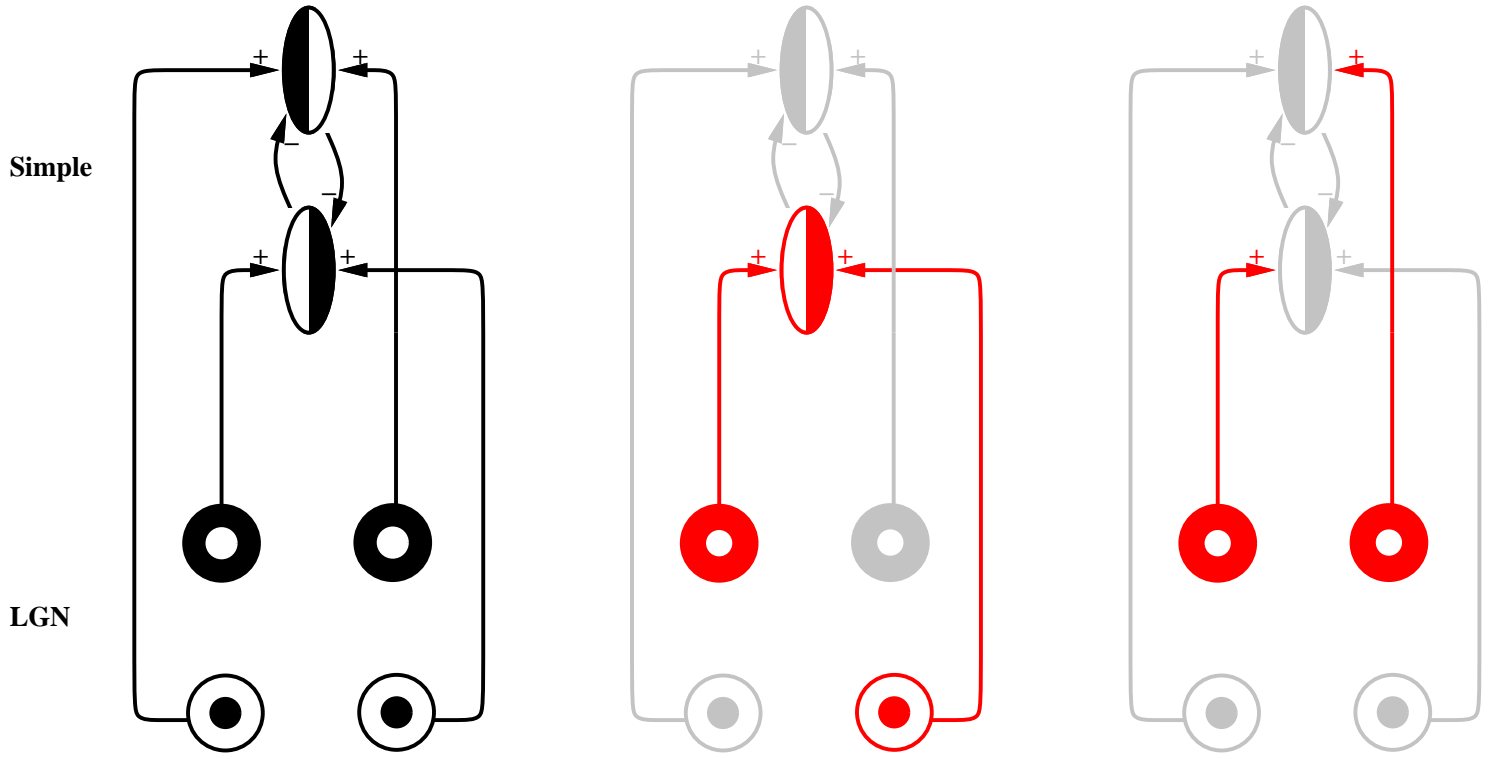


Figure 8:

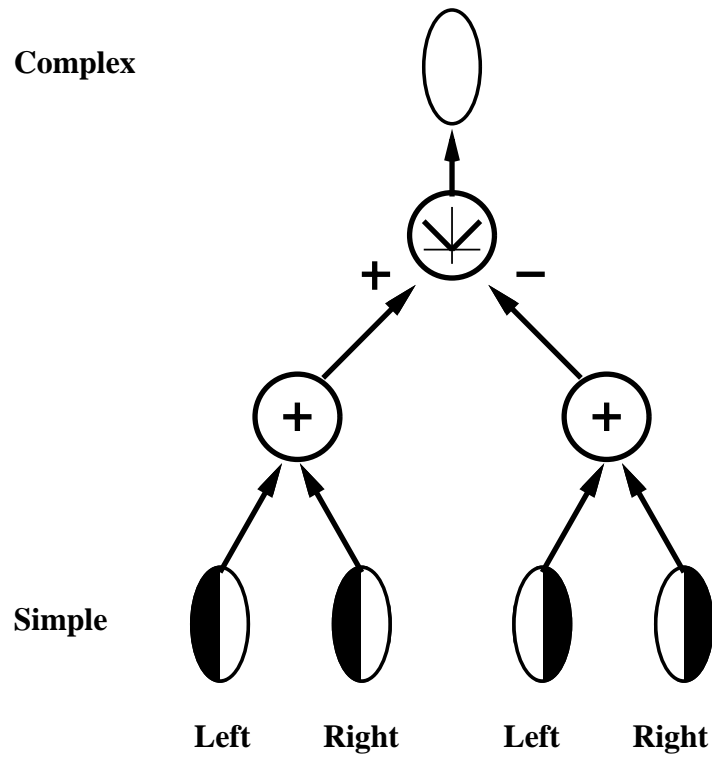
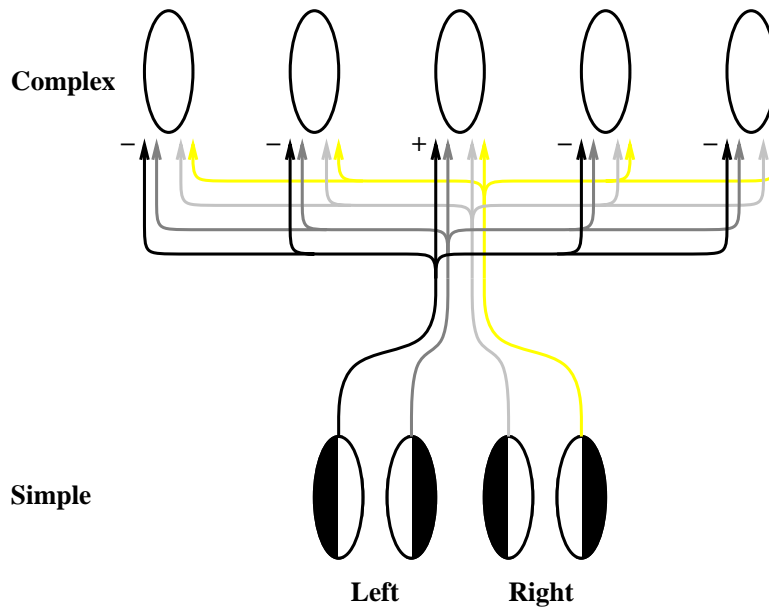


Figure 9:

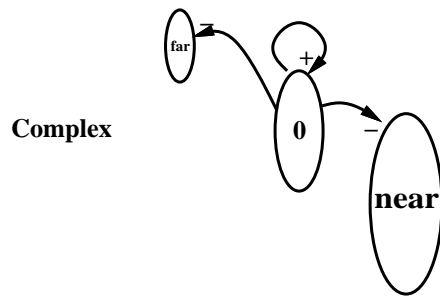
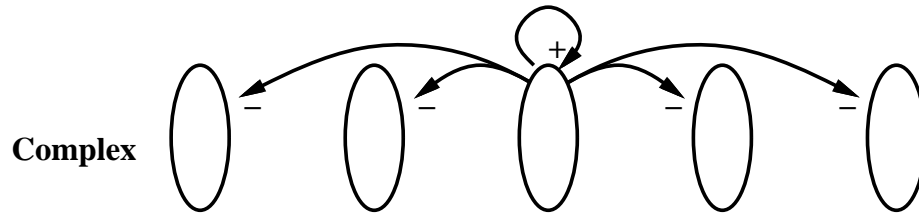


Figure 10:

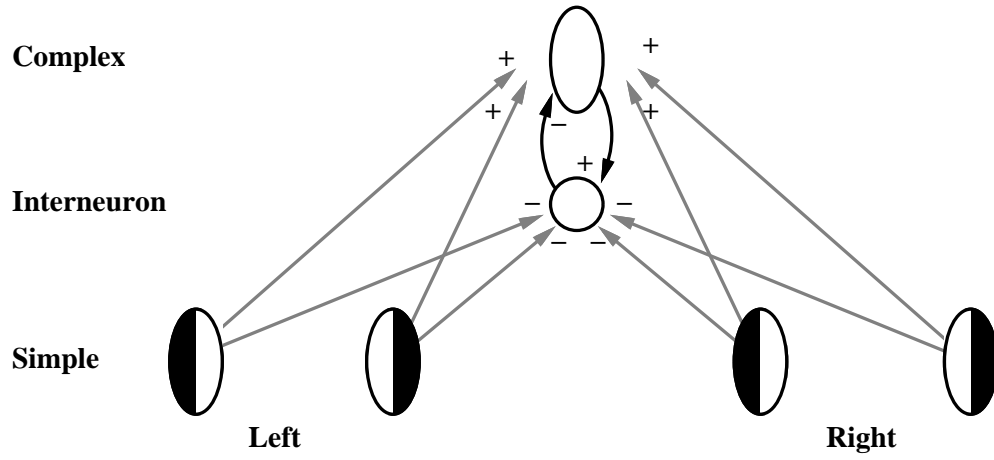


Figure 11:

DISPARITY PROCESSING

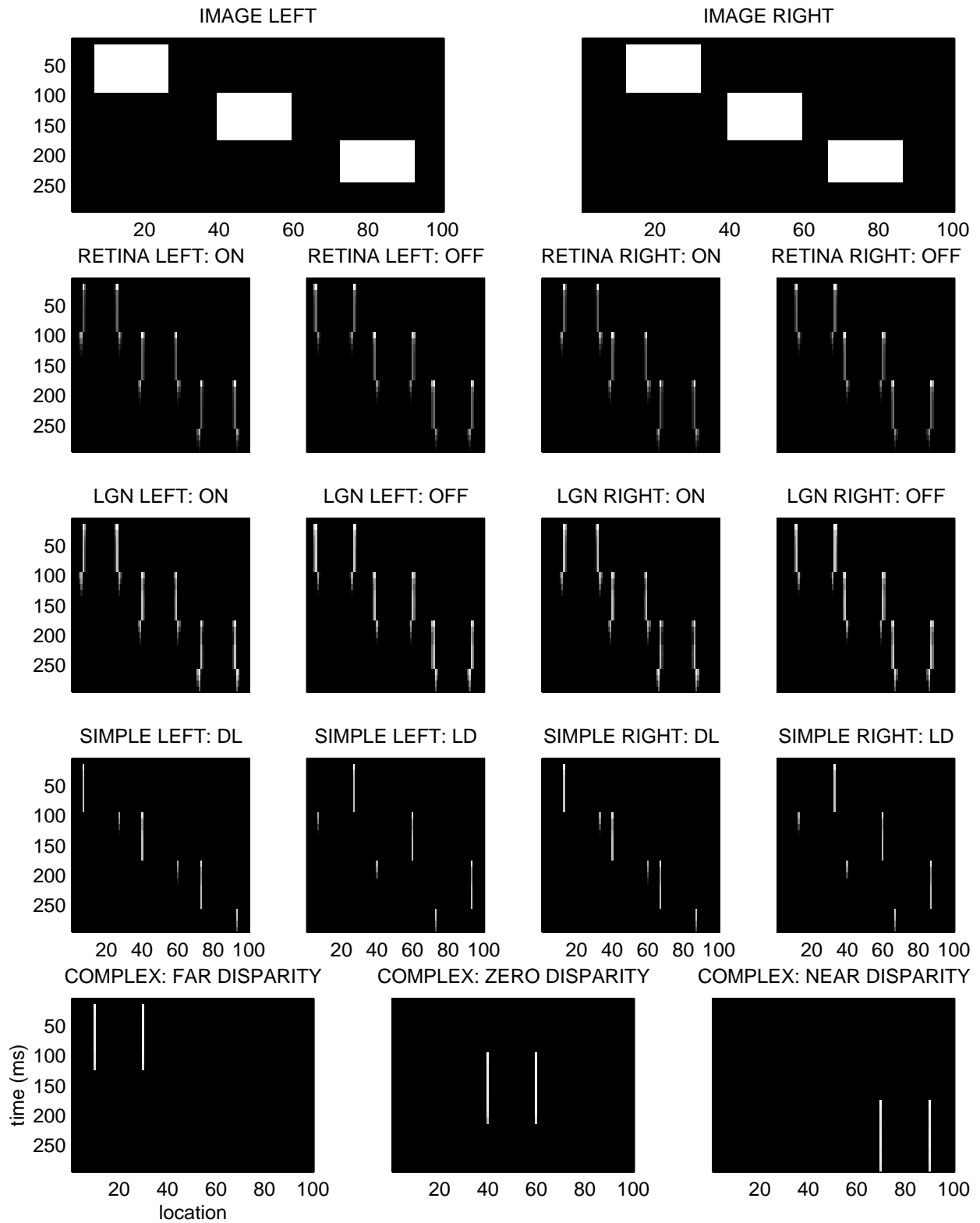


Figure 12:

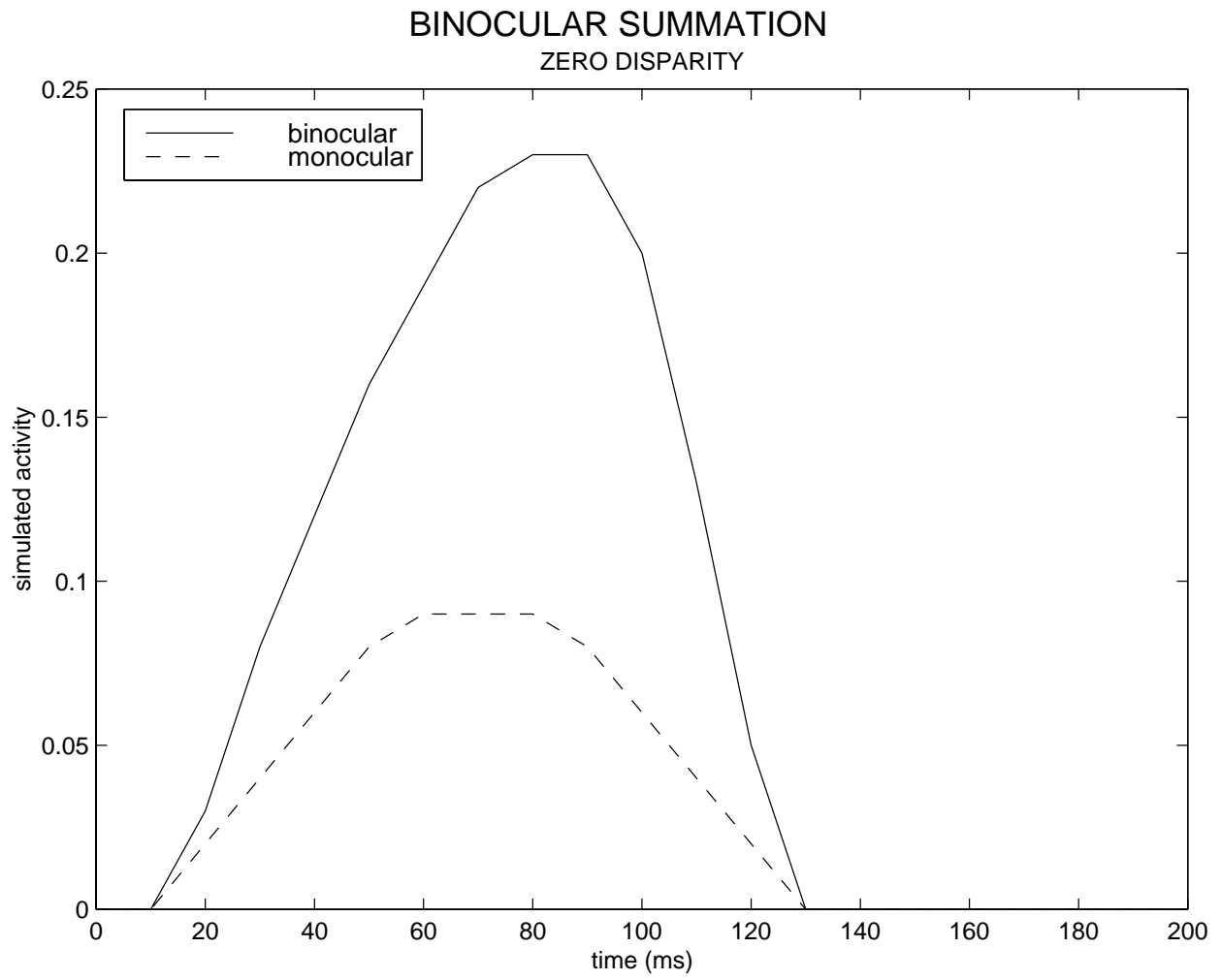


Figure 13:

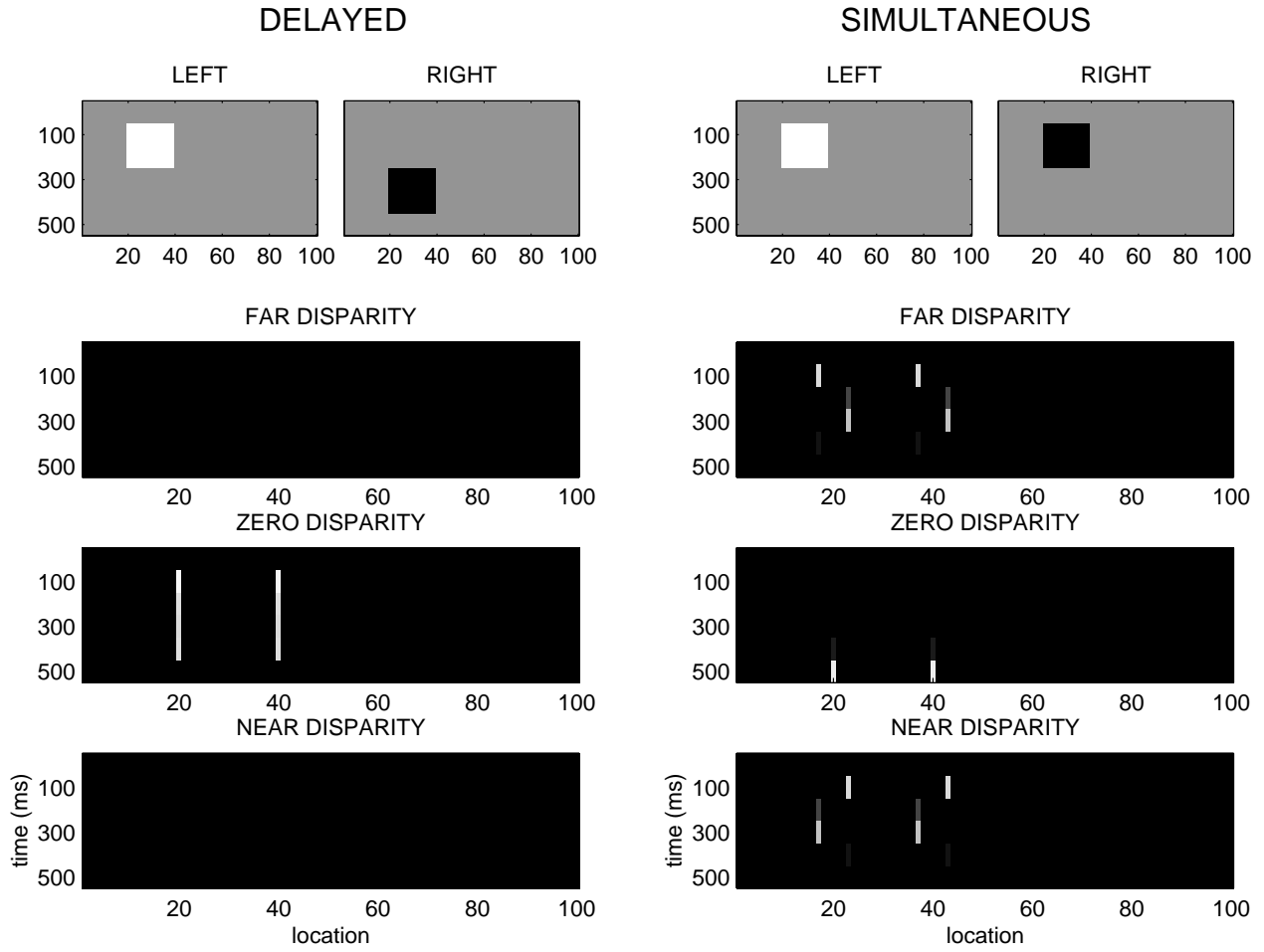


Figure 14:

IMPORTANCE OF CORTICOGENICULATE FEEDBACK

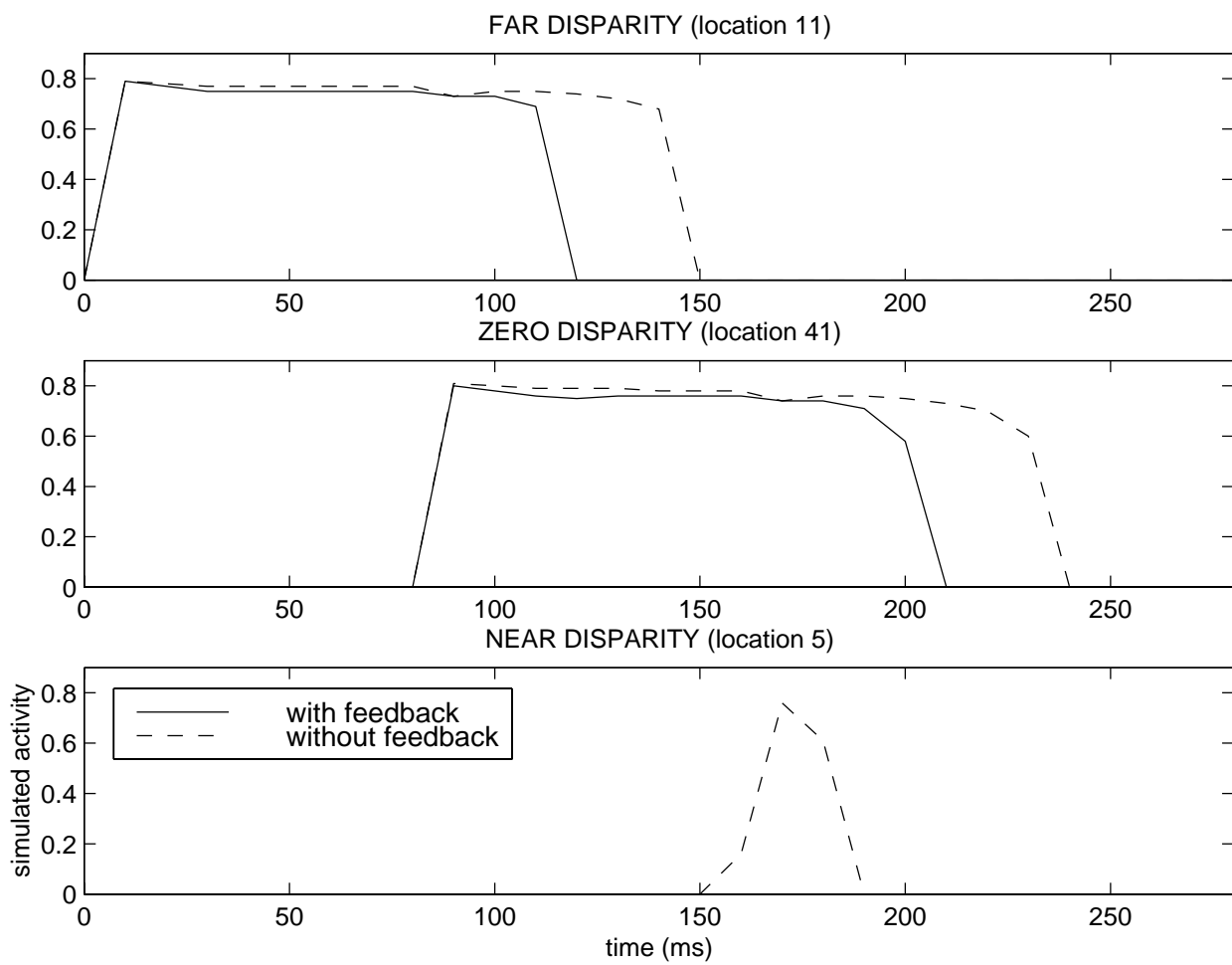


Figure 15: